Long-Range Forecasting and Climate Research

Statistical Prediction of NE Brazil seasonal rainfall from sea surface temperatures

by

M.N. Ward and C.K. Folland

LRFC 31

October 1989

Meteorological Office (Met. O. 13)
London Road
Bracknell
Berkshire RG12 2SZ

LONG RANGE FORECASTING AND CLIMATE RESEARCH MEMORANDUM NO 31

(LRFC 31)

STATISTICAL PREDICTION OF NE BRAZIL SEASONAL RAINFALL FROM SEA SURFACE TEMPERATURES

M N WARD AND C K FOLLAND

(Submitted to the International Journal of Climatology)

LONDON, METEOROLOGICAL OFFICE.
Long-Range Forecasting and Climate Research Memo.LRFC.31

Statistical prediction of the NE Brazil seasonal rainfall from sea surface temperatures.

06780190

551.509.324.2
551.509.331
551.526.6

MET O 13 (SYNOPTIC CLIMATOLOGY BRANCH)
METEOROLOGICAL OFFICE
LONDON ROAD
BRACKNELL
BERKSHIRE RG12 2SZ

OCTOBER 1989

Abstract

Two statistical methods are demonstrated for making seasonal forecasts of tropical rainfall; one method uses multiple linear regression (MLR) and the other uses linear discriminant analysis (LDA). MLR is used to forecast seasonal rainfall in standardised anomaly units. LDA makes a probability forecast for pre-defined anomaly ranges.

In this paper, the two methods are used to forecast the February to May NE Brazil rainfall season. Forecasts are made from pre-rainfall season values of Atlantic and Pacific sea surface temperature anomaly (SSTA) eigenvector coefficient time series; thus the results isolate that component of predictability that results from SSTAs alone. Models are constructed using half of the post-1911 historical data period, and test forecasts are made for the remaining years. The forecast skill is assessed in several ways, including a new score which measures the error linearly in probability space. The scores suggest that about 50% of the interannual NE Brazil rainfall variance is predictable from these methods, and that the forecasts have no significant bias. This level of skill over such a long period is a useful advance on previous attempts at forecasting NE Brazil seasonal rainfall and compares favourably with other promising attempts at prediction of seasonal rainfall in tropical regions.

SSTAs with a near world-wide coverage are today available in real-time, so it is possible to use the methods in this paper to forecast seasonal NE Brazil rainfall in real-time. Successful experimental forecasts produced prior to the main rainfall seasons of 1987 to 1989 are briefly reviewed.

key words seasonal forecasting, tropical rainfall, sea surface temperatures, eigenvectors

1. Introduction

The prospect of seasonal rainfall prediction for some tropical regions has advanced greatly in the last decade. Pre-rainfall season values of mean sea-level pressure, mean zonal and meridional surface winds and sea surface temperatures (SSTs) show strong relationships with seasonal rainfall indices for a number of tropical regions (Nicholls (1987), Hastenrath Wu and Chu (HWC, 1984), Hastenrath (1987), Hastenrath (1988), Parker et al (1988)). The state of the troposphere at middle and upper levels also appears to be a useful indicator of rainfall in some regions (eg for India, Bhalme et al (1986)), though the length of the historical record is much shorter and therefore conclusions are more difficult to draw. Similar comments apply to promising links between the quasi-biennial oscillation in the stratosphere and surface weather (Labitzke and van Loon, 1988) including tropical rainfall (Bhalme et al, 1987).

In addition to these empirical studies, theoretical studies and numerical models including General Circulation Models (GCMs) have advanced understanding of the tropical atmosphere (eg Gill and Rasmusson (1983), Palmer and Mansfield (1986), Krishnamurti et al (1987)). For interannual variability, studies suggest that boundary forcing is more important in the tropics than in the extra-tropics. For example, the importance of SST anomalies (SSTAs) in the observed low frequency variability of the tropics was suggested by the 15-year GCM integration of Lau (1985), and specifically for the Sahel by Folland and Owen (1988). This has lead to the possibility of using a GCM for seasonal forecasting in the tropics (Owen and Ward, 1989, Shukla and Fenessy, 1988).

The Brazilian states normally taken to define the N Nordeste (NE Brazil) extend over 35°-45° W, 2°-10° S (Fig 1). Most of the annual rainfall usually occurs in the months March and April when the inter-tropical convergence zone (ITCZ) is closest to, though still mostly to the north of, the Nordeste. There is substantial interannual variability in the seasonal rainfall anomaly averaged over the region (Fig 2). Previous studies have related this variability to the location of the ITCZ (eg Hastenrath and Heller,1977), indices of the Atlantic trade winds (in particular Chung,1982), the El Nino Southern Oscillation (ENSO) in the Pacific (Caviedes, 1973; Covey and Hastenrath, 1978) and sea surface temperature anomalies (SSTAs) in the tropical Atlantic (Markham and McLain,1977). The potential influence on N Nordeste rainfall of an SSTA north-south dipole in the tropical Atlantic was confirmed by forcing a GCM with such an SSTA pattern (Moura and Shukla,1981). Recently, Mechoso and Lyons (1988) showed that their GCM responded to the observed global SSTA pattern of boreal spring 1984 in a way that was consistent with much of the observed large scale circulation throughout the tropics and, specifically, the abundant rainfall in N Nordeste.

This paper empirically studies the relationships between NE Brazil seasonal rainfall and SSTAs, and develops and assesses

two methods of statistical prediction based on the relationships. In addition to SSTAs, the statistical models of HWC (1984) predicted N Nordeste rainfall from the pre-season measures of the Atlantic trade wind strength, N Nordeste rainfall and the Southern Oscillation Index (SOI). This had the advantage of including information not present in the SSTA fields, so the addition of non-SST predictors, including the sun spot cycle (Kane and Trivedi, 1988), may add further to our skill. However we use SSTAs alone here because there is strong evidence for a causal link between SSTAs and large-scale atmospheric circulation in the vicinity of N Nordeste from GCM experiments and because our SST data are believed to be adequate for analysis of large scale paterns back to about 1900 (Folland, Palmer and Parker (FPP), 1986) so that our forecast experiments can extend over a longer period than previously possible. Furthermore, using predictors which have a long historical record, but which are also available today in real-time, has allowed the production of experimental forecasts for each N Nordeste rainfall season since 1987. The results in this paper extend a preliminary study reported in Ward et al (1988).

Section 2 discusses the data used. Section 3 establishes the nature and statistical significance of SSTA-N Nordeste rainfall correlations, and demonstrates that a small number of eigenvector coefficient time series (EC time series) successfully expresses most of the link between SSTAs and N Nordeste rainfall. However, further analyses suggest that the all-seasons unrotated Atlantic eigenvectors used in section 3 rather over-simplify Atlantic SSTA variability. These analyses, and consequent improvements to rainfall predictability, are beyond the scope of this paper. Section 4 uses pre-rainfall season values of the Atlantic and Pacific EC time series as candidate predictors for Linear Discriminant Analysis (LDA) and Multiple Linear Regression (MLR) models. Very simple models using just one or two predictors are used so the two statistical forecasting methods can be illustrated clearly.

In Section 5 the statistical models are constructed using half the available historical data period (the 'model training period'), and forecasts are made and verified for the remaining half. A discussion and analysis of several methods of forecast verification is given so that comparison between results presented here and those of other papers is made easier.

2. Data

a) SST data

SST data are taken from the Meteorological Office Historical SST dataset version 3 (MOHSST3) which contains monthly SSTs, when available, for $5^{\circ}x5^{\circ}$ grid squares over the world's oceans. The data extend back to 1856, but this study is restricted to analysis of post-1900 data. The data have been corrected for changes in observational practice prior to 1942 in the way described by Parker and Folland (1988) and in more detail by Bottomley et al (in press).

After conversion to anomalies relative to a month by month 1951-80 climatology, the data were combined into a 10°x10° dataset. For analysis of large-scale SSTA patterns, the improved data coverage and reduced noise of a 10°x10° dataset outweigh loss of spatial resolution. Fig 3 shows that in fact a 10°x10° resolution is a good choice, since adjacent squares correlate well, and the correlations gradually decay with increasing distance (Morgan, Coventry Polytechnic undergraduate project, personal communication). For a particular month, a 10°x10° anomaly was included in this monthly dataset (dataset M) if any of the constituent 5°x5° squares had data.

The monthly data were then averaged into three month seasons (forming dataset S). One constituent month was required to be present for a seasonal anomaly to be calculated. Finally a seasonal dataset with all missing data interpolated (dataset SI) was constructed for the years 1901-1980. For inclusion in dataset SI, a 10°x10° square was required to have more than 60% of non-interpolated seasonal data present in dataset S over 1901-1980. For the squares included, the number of seasons present in each of the four twenty year periods is shown in Fig 4. Interpolations were made by fitting Chebyshev polynomials in time (eg see Burden and Faires, 1985). These estimates were combined with linear spatial interpolations in particularly data sparse situations (not applied in Ward et al, 1988).

b) Rainfall data

The standardised anomaly series of N Nordeste seasonal rainfall used in this study (Fig 2) is based on C Nobre's February to May series for 1912-1981 (Nobre, personal communication, series not yet available after 1981) and on updated values of HWC's March-April series for the years 1982-1985 (Lamb, Peppler and Hastenrath, 1986, and Hastenrath, personal communication). Nobre's series covers a larger area than that used by HWC (see Fig 1) and includes data from more stations (113 v 30). For 1913-1981 (the years for which both series are available) the two series correlate at 0.83 and the means and variances of the two series are almost identical. Correlations between SSTA eigenvector coefficient time series and the HWC series (and a series combining March-May rainfall data from just Quixeramobim and Fortaleza) were shown in Ward et al (1988) to not differ significantly from those achieved using Nobre's more comprehensive series.

3. Links between N Nordeste rainfall and Sea Surface Temperatures

a) Simple correlation studies

Fig 5a shows the correlations between March-May seasonal SSTA in each 10°x10° area in dataset S and N Nordeste rainfall for the years 1912-85. The statistical significance of each individual correlation has been estimated using a standard t-test since there are no significant serial correlations in the N Nordeste rainfall series (see Katz, 1988 for a discussion of the problems

caused by large serial correlations in both of the series being correlated). The pattern of correlations in the tropical Atlantic is consistent with the findings of Markham and McLain (1977) with strong positive correlations in the south tropical Atlantic, and negative correlations in the north tropical Atlantic. Significant negative correlations extend north into the extra-tropics towards Greenland; this is consistent with Namias (1972) who inferred from 700mb geopotential height data that an interaction with the N Atlantic extra-tropics was involved in N Nordeste rainfall variability. The negative correlations in the tropical Pacific extend over a wide area and provide strong evidence for the relationship between El Nino (La Nina) and drought (flood) in N Nordeste that had been previously suggested from analysis of the Southern Oscillation Index and SSTAs along the coasts of Peru and Ecuador (eg Covey and Hastenrath, 1978).

Care must be taken when interpreting maps of correlations with local SSTA time series because the SSTAs have strong spatial correlations. The spatial correlation results in an increased chance of a large proportion of the analysis area being covered in significant correlations. To estimate the field significance of the map we have estimated the likelihood of achieving by chance the proportion of significant area in Fig 5a using a Monte Carlo experiment (see Livezey and Chen, 1983). For the experiment, 500 time series were simulated by randomly rearranging the values in the 1912-1985 N Nordeste rainfall series. These series were correlated with March-May SSTAs for 1912-1985, producing 500 correlation maps of the type shown in Fig 5a. None of the 500 had as much area as Fig 5a covered with significant correlations, so the result in Fig 5a is very unlikely to be the product of chance ie the field is statistically significant at <1% level.

The similarity between correlation maps calculated for 1912-48 and 1949-85 (Figs 5b and 5c) in the tropical Atlantic and Pacific supports the idea that the correlations in these regions are based on recurring physical relationships in the ocean-atmosphere system. Though the correlations with the tropical Indian ocean are weak, they are also similar in the two periods. It is likely that the associations are real and due either to Indian Ocean SSTAs moving in phase with SSTAs in that part of the Pacific Ocean that forces atmospheric changes in the vicinity of NE Brazil, or to the Indian Ocean SSTAs playing a role in the forcing of the important atmospheric changes, perhaps in partnership with the Pacific SSTAs. The role of the Indian Ocean is an area for future investigation. In the N Atlantic extra-tropics the pattern of correlations is weaker in the earlier period. The atmosphere behaved unusually in this sector in the 1920's and 1930's and there was also a dramatic warming of the N Atlantic (Rogers, 1985). The relationship between these events and the correlations in Fig 5c also requires future investigation.

(b) SSTA eigenvectors

A linear transformation was applied to the SSTA data (dataset SI) in the Atlantic Ocean and (separately) in the Pacific Ocean. The main purpose was to try to derive a few time series which express much of the large-scale variability in the SSTA data in these regions. For example, one such derived time series may trace the variability in El Nino / La Nina, enabling much of the Pacific correlations in Fig 5 to be succinctly expressed by the correlation between one time series and N Nordeste rainfall.

Let the matrix of SSTA data (either for the Atlantic or Pacific) be denoted by the matrix $\mathbf{x}$. For the Atlantic, this contains 94 time series of SSTAs for the 320 seasons in the period 1901-80 For the Pacific, just winter (Dec-Feb) data are used in the 126 time series (see appendix I for further discussion). $\mathbf{x}$ is transformed to produce $\mathbf{Z}$ which contains the same number of time series as $\mathbf{x}$:-

$$\mathbf{Z} = \mathbf{A}^T\mathbf{x} \qquad (1)$$

In the transformation used here, the kth column, α_k, of the matrix $\mathbf{A}$ is the kth eigenvector of the covariance matrix of $\mathbf{x}$. Defining $\mathbf{A}$ in this way results in the first row of $\mathbf{Z}$ (z_1, the first eigenvector coefficient (EC) time series) having maximum variance, z_2 having maximum variance subject to orthogonality with the first row, and so on (see Jolliffe,1986).

Each eigenvector α_k has a term or weight, a_{ki}, for each grid-square in the analysis domain, so the weights can be plotted in the form of spatial patterns.

Once the eigenvectors described above have been derived, further time series can be formed:

$$\mathbf{Z}_n = \mathbf{A}^T\mathbf{x} \qquad (2)$$

where $\mathbf{x}$ is any set of Atlantic (Pacific) SSTA fields and the $\mathbf{A}^T$ are the Atlantic (Pacific) eigenvectors derived above. The $\mathbf{Z}_n$ time series trace the history of the modes of SSTA variability described by the corresponding $\mathbf{A}^T$ patterns. For example monthly data may be used in $\mathbf{x}$ to yield $\mathbf{Z}_n$ time series with a monthly rather than seasonal time resolution.

Orthogonal rotation of the first few α_k will maintain the collective variance in the corresponding $\mathbf{z}_k$, and may produce eigenvector patterns which more closely resemble real patterns of variability, providing the rotation criteria are sensibly chosen (Richman, 1986). Results of such analyses, or non-orthogonal rotations, are beyond the scope of this paper. As we shall show, in this particular case they are not essential to illustrate the potential of the eigenvector approach for succinctly expressing links between SSTAs and NE Brazil rainfall. However, further research with rotated eigenvectors of Atlantic and Pacific SSTA is justified.

Table I gives the variance of the first few EC time series, expressed as a percentage of the total variance in the Atlantic

or Pacific datasets. Using a test discussed by North et al (1983) the variances accounted for by Atlantic eigenvector 3 (AV3) and Atlantic eigenvector 4 (AV4) are sufficiently similar to cast doubt on the statistical significance of the patterns. However, while AV3 is related to N Nordeste rainfall, AV4 is not (see below), so the distinction between them is probably physically real.

Table I Percentage of variance accounted for by first seven covariance eigenvectors of Atlantic (all seasons) and Pacific (Dec-Feb season) seasonal SSTA 1901-1980.

	EIGENVECTOR NUMBER							
	1	2	3	4	5	6	7	total
Atlantic	15.2	8.2	6.8	6.5	4.8	3.8	3.3	48.6
Pacific	16.5	10.8	6.6	5.4	4.1	3.7	3.4	50.5

Fig 6a shows that the first Atlantic eigenvector (AV1) has everywhere weights of the same sign, so the EC time series (AT1) traces overall warming and cooling in the Atlantic. Fig 6b shows that warming in the Atlantic through this century took place mainly in the 1920's and 1930's. AV1 is quite like the Atlantic part of eigenvector 1 for global SSTAs shown in Folland and Colman (1988) and Parker and Folland (1989).

AV2 (Fig 7) is mainly a bi-polar pattern (positive in the S Atlantic, negative in the N Atlantic), but with areas near NW Europe and the Gulf of Mexico in opposition to the rest of the N Atlantic. A bi-polar second eigenvector can be an artifact (Richman,1986), but this pattern may here have a physical significance, being the Atlantic part of a near worldwide mode of variability (related to interdecadal variations in Sahel rainfall) where the N Atlantic and N Pacific warm/cool out-of-phase with the S Atlantic and Indian Oceans (see Folland and Colman, 1988 and Parker and Folland, 1989)

In AV3 (Fig 8a) weights are strongest in the south Atlantic, where the Benguela current, and much of the S tropical Atlantic show weights out of phase with the rest of the S Atlantic and most of the N Atlantic. The pattern of weights resembles the inverse of the Atlantic correlation patterns in Fig 5, suggesting that AT3 should be negatively correlated with N Nordeste rainfall. This is confirmed for March-May values of AT3 in Fig 8b and Table II. No other EC time series correlates so strongly, though AT2 and AT7 also have statistically significant correlations.

The first Pacific eigenvector (PV1, Fig 9a) has weights which resemble the pattern of SSTAs during an El Nino event. PT1 traces the history of El Nino (very positive values of PT1) and La Nina (very negative values of PT1) through the present century. This is indicated by a correlation of 0.82 between a Dec-Feb time

Table II Correlations for 1912-85 between N Nordeste rainfall and March-May values of Atlantic and Pacific eigenvector coefficient time series.

	Eigenvector Number						
	1	2	3	4	5	6	7
Atlantic	-0.08	0.36	-0.54	-0.02	-0.15	0.01	0.26
Pacific	-0.40	-0.01	-0.03	0.23	0.09	-0.04	0.27

Note: assuming 60 degrees of freedom, correlation significance thresholds are
5% : r = +/- 0.25
1% : r = +/- 0.32

series of SSTA in the east tropical Pacific (10N-15S, 140-160W) and PT1. To relate the eigenvector pattern to N Nordeste rainfall, we calculate a March-May EC time series for PV1 by using, in Eq 2, the Pacific eigenvectors in $\mathbf{A}^T$ and March-May data in $\mathbf{x}$. The March-May PT1 values and N Nordeste rainfall are plotted together in Fig 9b; the correlation between the two is statistically significant (see Table II).

PV2 (not shown), like AV1, reflects in phase warming and cooling across the analysis domain; PT2 shows no association with N Nordeste rainfall. Of the remaining Pacific eigenvectors, none have time series that show very significant correlations with N Nordeste rainfall.

Large scale SSTA patterns do not usually change very much over a few months, suggesting that pre-rainfall season values of EC time series, in particular AT3 and PT1, may be useful predictors of N Nordeste rainfall. To examine this, further EC time series were formed using data from the monthly dataset M for $\mathbf{x}$ in Eq 2, and these series were correlated with N Nordeste rainfall at various lead times. To reduce sampling error, EC time series values for adjacent months were averaged for the correlations with AT3 and PT1 shown in Fig 10. With increasing lead time (ie time before the rainfall season), the correlation with PT1 slowly declines to a level that, by Nov-Dec, is marginally significant at the 5% level. For AT3, the correlations are still statistically significant at the 1% level when July-August values are used, a lead time of six months on the N Nordeste rainfall season. The AT3 correlations do however decline quite rapidly from the value in January-February to the value in November-December. This is now investigated.

Eq 2 can be written as a summation for each eigenvector k and for each time period j:

$$z_{jk} = \Sigma_i a_{ik} x_{ij} \qquad (3)$$

where i indicates the grid square and summation is over all grid

squares in the analysis domain. Now consider forming for a given time period j and each Atlantic eigenvector k:

$$z(t)_{jk} = \Sigma_{i_t} a_{ik} x_{ij} \quad \text{and} \quad z(ne)_{jk} = \Sigma_{i_{ne}} a_{ik} x_{ij} \qquad \text{(4a and 4b)}$$

where i_t indicates summation over only tropical squares (30N to 30S) and i_{ne} indicates summation over extratropical squares north of 40°N. The two time series so formed when k = 3, AT3(t) and AT3(ne), can be viewed as tracing the tropical (t) and N extra-tropical (ne) signals of AV3. The correlations of these two series with N Nordeste rainfall are plotted in Fig 11. The AT3(ne) series correlates significantly (at the 1% level) during the N Nordeste rainfall season, but the correlations quickly become insignificant when the series leads the rainfall season. In contrast, AT3(t) shows strong lead correlations, and thus appears a more powerful predictor than an EC time series for the whole Atlantic, as used in Ward et al (1988).

4. Methods of forecasting

Section 3 suggests that it may be possible to skilfully predict N Nordeste seasonal rainfall totals from the SSTA patterns observed in the months preceeding the rainfall season. To produce a statistical forecast method usually requires the following steps:

a) Choose the predictand. Here it is the seasonal rainfall.
b) Choose the candidate predictors. Here they are the pre-rainfall season SSTA EC time series values.
c) Choose a statistical technique for constructing a forecast model that relates the predictors to the predictand.
d) Choose a period (the training period) to provide the data for estimating the model parameters, which express the relationships between predictors and predictand.

The two forecast methods presented below handle steps a) and c) very differently. Different advantages and disadvantages result.

METHOD 1 Multiple Linear Regression (MLR) statistical technique

This statistical technique was also used by HWC (1984) to predict N Nordeste rainfall. The predictand is the standardized rainfall anomaly, and the forecast is usually interpreted as a 'point estimate' ie a precise forecast of the standardised rainfall anomaly, though conversion to a probability forecast is possible and is discussed later. The statistical forecast model is

$$R = b_0 s_0 + b_1 s_1 + b_2 s_2 + \ldots\ldots\ldots + b_p s_p + e \qquad (5)$$

where R is rainfall in standardized units, s_i is the value of the i^{th} predictor in the model (s_0 always equals 1), b_i are the true model parameters representing the true relationship between the predictors and predictand, p is the number of predictor variables in the model and e is the unmodelled variance in the rainfall series. The b_i must be estimated from the relationships in the

training period data. The term e is always unknown, but if assumed to be normally distributed with mean zero, then the best estimate of the predictand is (writing the b_i and s_i as column matrices)

$$R' = \mathbf{B}'\mathbf{s}^T \quad (6)$$

where R' is the predicted rainfall, and **B'** are the estimates of the model parameters, chosen to minimize $\Sigma\ (R'-R)^2$, where summation is over the training period.

The best estimate of the variance of e is

$$\text{var}(R-R') = \sigma_e^2 = \frac{\Sigma\ (R-R')^2}{N - (p+1)} \quad (7)$$

where p+1 is the number of fitted model parameters and N is the number of years in the training period.

Ignoring error in the estimation of **B'**, the standard error (SE) of a prediction is σ_e, but when the **B'** errors are also considered, the SE of a prediction increases to (in matrix notation, see Weisberg,1976 for a derivation)

$$SE^2 = \sigma_e^2(\mathbf{s}^T(\mathbf{S}^T\mathbf{S})^{-1})\mathbf{s}) \quad (8)$$

where **s** is the vector of variables being used for the current prediction and **S** is the N x (p+1) matrix of training period predictor data (the p+1 columns comprise the p variables $s_1 \ldots s_p$ in the model and a column of 1's for s_0). The proportion by which σ_e^2 is raised in eq 8 depends on the variances and covariances in the predictor training data and on the amount by which the predictors for the current prediction differ from their average values. For the two-variable models discussed below and in Section 5.2, the SE is usually raised by about 10% above σ_e^2, with the SE varying by about 5% over different predictions. For models with more predictors and larger covariances among the predictors, the changes become larger.

The predictor variables for the forecast model may be selected from a set of candidates either using objective methods or from an exploration of the relationships between predictors and predictand. The objective method used here is stepwise multiple regression which chooses the next predictor to enter into the model on the basis of the proportion of unexplained variance σ_e^2 that is explained by each of the candidate predictors not yet in the model. A threshold statistical significance α_t is set which a variable must exceed if it is to be entered into the model.

To illustrate the MLR technique, a forecast model is fitted using a 1912-81 training period. The 14 candidate EC time series predictors are formed by using Dec-Feb seasonal SSTA fields for the whole Pacific (forming 7 PT series) and the tropical Atlantic (forming 7 AT(t) series). Models constructed using α_t = 1% (Eq 9a) and 5% (Eq 9b) are:

$$R' = 7.2 - 58.0(AT3(t)) - 8.7(PT1) \quad (9a)$$
$$R' = 3.8 - 87.8(AT3(t)) - 8.0(PT1) - 9.2(PT3) - 68.0(AT5(t)) \quad (9b)$$

The model parameters for PT1 (El Nino eigenvector) look small, but the contribution of PT1 to the forecast R' is not usually so small because the standard deviation of PT1 is greater than that of other predictors. The standard deviation of (8.7 x PT1) is 26.9 and of (58.2 x AT3(t)) is 47.6, suggesting AT3(t) is on average twice as important as PT1 in determining the forecast from the statistical model in Eq 9a. However, either predictor may dominate in a particular year.

Fitting the model parameters to minimize $\Sigma(R-R')^2$ results in the standard deviation of the model forecasts (σ_f) being less than the standard deviation of the observed values (σ_v); it is easy to derive that the ratio of σ_v to σ_f is given by

$$\sigma_f = \sigma_v r \quad (10)$$

where r is the correlation between the forecast and observed values in the training period. Thus a moderate relationship between the predictors and the predictand will rarely produce forecasts of extreme values. A possible response to this is to apply a correction to the forecasts to increase the expected standard deviation of the forecasts to approximately σ_v which, from Eq 10, can be achieved:

$$R'_{inf} = (R' - \mu_v)r^{-1} + \mu_v \quad (11)$$

where R'_{inf} is called the inflated regression prediction, and μ_v is the average of the predictand in the model's training period. Inflated regression forecasts are tested later along with conventional regression predictions.

An alternative way to overcome the low variance in the MLR predictions is to interpret them as probability forecasts rather than point estimate forecasts, using the fact that the conditional distribution of the predictand is approximately normal with mean R' and standard deviation SE (Lindley, 1965). MLR probability forecasts for NE Brazil rainfall are discussed in Section 5.2e.

METHOD 2 Linear Discriminant Analysis (LDA) statistical technique

For this method, each rainfall season is categorized on the basis of its position in the cumulative distribution of the standardised anomaly rainfall index. In the results presented here (and in Ward et al 1988, and Parker et al 1988), the driest 20% of seasons in the model's training period are allotted to category 1, the next driest 20% to category 2 etc. This defines five equiprobable categories (quints). LDA models are constructed to forecast the probability of each category. The categories were chosen mainly in an attempt to distinguish very dry seasons (driest 20%) from very wet seasons (wettest 20%).

LDA uses Bayes Probability Theorem and estimates the posterior (forecast) probability of category i given a column matrix of predictors (see Afifi and Azen, 1979). For just one predictor, x, the probability of quint i given x is

$$Pr(Q_i/x) = \frac{q_i f_i(x)}{\Sigma q_j f_j(x)} \qquad (12)$$

where summation is over all five categories

q_i = prior probability of category i (if the categories are quints, each has a prior probability of 0.2, and the q_i cancel in Eq 12)

$f_i(x)$ = probability of observing predictor variable x when Q_i is observed. $f_i(x)$ can be regarded as a probability density function.

The problem described by Eq 12 is illustrated in Fig 12. This shows, for the years 1912-81, the estimated distributions of the Dec-Feb value of AT3(t) for each of the N Nordeste rainfall quints. The distributions are assumed to be Gaussian. The standard deviation of all the distributions is assumed to be the same, and is a pooled estimate. The mean, μ_i, of each distribution is estimated from the values of AT3(t) in the n = 14 years categorised as quint i in the training period. Note that MLR did not require so many parameters to be estimated from the training period, and all parameters were estimated from the full set of years so limiting sampling error. For this example, each μ_i has a standard error of about $\sigma/\sqrt{n} = 0.66/\sqrt{14} = 0.18$. Fig 12 shows that μ_2 and μ_3 differ by only 0.04, so that sampling error clearly dominates any signal. This is often found for the central three quints and future formulations of the forecast method could consider the benefits of combining these categories into one or two central ranges. In contrast, μ_1 and μ_5 are significantly different (at the 5% level according to a t-test) from the value of respective adjacent means in Fig 12.

For the observation A on Fig 12, Eq 12 yields the probability of quint 5 to be

$$Pr(Q_5/x) = \frac{0.38}{0.01 + 0.09 + 0.08 + 0.18 + 0.38} = 0.51$$

The probabilities of the other quints are estimated in the same way (see Fig 12). Thus a one-predictor LDA model can be set up in a very simple way.

Usually we want to forecast the probability of each category (quint) using more than one predictor variable. To do this we must consider the multivariate distributions of the predictor variables. In LDA the distributions are assumed to be multivariate normal. Given p normally distributed predictor variables then the log of the multivariate probability density function of **X** for quint i is

$$\ln(f_i(\mathbf{X})) = \alpha_{i1}x_1 + \alpha_{i2}x_2 + \ldots\ldots\alpha_{ip}x_p + \Gamma_i \qquad (13)$$

$$\begin{bmatrix} \alpha_{i1} \\ \cdot \\ \cdot \\ \alpha_{ip} \end{bmatrix} = \boldsymbol{\Sigma}^{-1}\boldsymbol{\mu}_i \ , \qquad \Gamma_i = -\tfrac{1}{2}\boldsymbol{\mu}_i^T\boldsymbol{\Sigma}^{-1}\boldsymbol{\mu}_i$$

where $\mathbf{X}$ = vector of observed predictor variables $x_1, \ldots\ldots x_p$
$\boldsymbol{\Sigma}$ = covariance matrix of the predictor variables in the training period
$\boldsymbol{\mu}_i$ = vector containing the mean value of each predictor variable in those years when quint i is observed in the training period.

Substituting Eq 13 into Eq 12 yields the multivariate LDA probability equation

$$\Pr(Q_i/\mathbf{X}) = \frac{\exp(d_i)}{\Sigma \exp(d_j)} \qquad (14)$$

where d_i, called the discriminant score for category i, is

$$d_i = \alpha_{i1}x_1 + \alpha_{i2}x_2 + \ldots\ldots\alpha_{ip}x_p + \Gamma_i + \ln(q_i) \qquad (15)$$

Like MLR, a subset of the candidate predictors must be chosen for inclusion in the model. The most common objective stepwise method uses a one-way analysis of variance to assess the statistical significance of each predictor. However, this is not appropriate in this application because the test ignores the fact that the categories are ranges taken from a continuous distribution. Results from stepwise MLR and section 3 are used to guide LDA model selection.

5. Assessment

5.1 An introduction to the skill scores

The skill of a forecast or of a set of forecasts can be measured in many ways. This paper uses a number of scores chosen because they each give most weight to different attributes of the forecasts.

Skill scores are often scaled so that a set of perfect forecasts score 100% and a 'reference forecast strategy' (RFS) scores 0%. This helps in comparing different sets of forecasts. Frequently used RFSs include
(i) climatology ie a forecast of the mean rainfall,
(ii) persistence ie the forecast for year j is the rainfall that was observed in year j-1,
(iii) chance ie the average score that would be achieved by randomly selecting a forecast value from the frequency distribution of the observed values in some reference period.

Chance is used as the RFS in some scores below, with persistence and climatology being viewed as alternative forecast strategies whose score could be considered separately.

a) scores for forecasts made on a continuous scale
Forecasts from the MLR technique are on a continuous scale.

Correlation
Correlation assesses a set of forecasts. It is calculated using the standard correlation formula:

$$r_f = \frac{\Sigma\, f'v'}{N(\sigma_f\sigma_v)} \qquad (16)$$

where f' and v' are deviations of the forecast from the forecast mean and observed from the observed mean. Summation is over the N forecasts being assessed and σ_f and σ_v are the standard deviations of the forecast and observed values. The score takes values between -1 and +1. The expected value of r_f from chance is 0, so the score automatically uses chance as the RFS. The score for climatology forecasts is also 0, since f'= 0 for all forecasts. Persistence forecasts may score well. The correlation score could be transformed to use persistence as the RFS (Daan,1984). Instead, we present in section 5.2 the correlation score achieved by persistence forecasts (r_p) to assess whether our forecast methods perform better than persistence.

The correlation is a measure of the linear association between the forecast and observed series. The score ignores any bias in the mean forecast value and the slope of the linear association between forecast and observed. Thus other scores are needed to check for these problems.

Root Mean Square error (RMS) and bias
These scores have been widely used in assessing seasonal rainfall forecasts for tropical regions (eg Hastenrath,1987 Nicholls,1984). They are defined:

$$\text{RMS} = \left[\frac{\Sigma(f-v)^2}{N}\right]^{\frac{1}{2}}$$

$$\text{BIAS} = \frac{\Sigma\,(f-v)}{N} = \mu_f - \mu_v$$

where Σ is over the N forecasts, f is the forecast and v is the observed. The scores do not, as formulated here, indicate skill relative to a RFS.

RMS has a special relationship with least squares regression, since it is the quantity that the model parameters are chosen to minimise. RMS can be expanded and written as

$$RMS = \left[(\sigma_f)^2 + (\sigma_v)^2 - 2\sigma_f\sigma_v r + (BIAS)^2 \right]^{\frac{1}{2}} \quad (17)$$

so the score is a function of correlation, bias, σ_f and σ_v. Until the correlation approaches 1 or the bias become very large, the contribution to RMS from bias remains quite trivial.

The dependence of RMS on σ_v and σ_f in Eq 17 implies that
(i) RMS scores cannot be compared for different sets of forecasts if σ_v differs greatly.
(ii) For a given low r_f, the score can be improved by simply reducing σ_f. For example, if forecasts are made with $\sigma_f=\sigma_v$, then r_f must be >0.5 for the RMS score achieved by climatology forecasts to be improved upon (see Eq 17). For most purposes, a set of forecasts that have r_f = 0.5 would be more useful than forecasts of climatology. The mean absolute error, widely used as a skill score (eg Nicholls, 1984)), is very similar to RMS and also suffers from the above problems.

BIAS can be useful for comparison of different sets of forecasts if its statistical significance is also offered.

Linear Error in Probability Space for continuous predictand, LEPS(cont)
An alternative approach is to compare the position of the forecast and observed values in the cumulative probability distribution of the observed values (see Fig 13). In Fig 13, the distance between the forecast standardised rainfall value -25 and observed value -50 is, in probability space, p(R<-25) - p(R<-50) = 0.39 - 0.19 = 0.20. A skill score that has a maximum value when the forecast and observed are coincident is:

$$S=1-a \quad (18)$$

where $a = \text{mod}(p_f-p_v)$ and p_f and p_v are the cumulative probabilities of the observed and forecast values. S will take values from 0 to 1. For a particular forecast and observation with cumulative probability p_f and p_v respectively, the expected score from chance is (see Appendix II)

$$\mu_s = 1.5(p_f - (p_f)^2 + 0.5)(p_v - (p_v)^2 + 0.5) \quad (19)$$

So the normalized score with a chance value of zero for each forecast is

$$S' = S - \mu_s \quad (20)$$

For the p_f and p_v marked on Fig 13, μ_s= 0.72 and S = 0.80, so S' = 0.08. For a perfect forecast ($p_f=p_v$= 0.19) μ_s= 0.64, so the score (S'_p) for a perfect forecast would have been 0.36. The LEPS percentage score for a set of continuous variable forecasts is

$$LEPS(cont) = \frac{\Sigma S' \times 100}{\Sigma(S'_p)} \qquad (21)$$

Note that when $(\Sigma S') < 0$ the forecasts have scored worse than the chance level; the denominator in Eq 21 should be the sum of the worst possible scores and the percentage score is treated as negative. This ensures that the score can take values from -100% to +100%.

For the forecast assessments in Section 5.2, the model training period's cumulative rainfall distribution is used for estimating p_f and p_v.

b) Scores for forecasts made on a categorical scale
For these scores, the LDA forecast is the category predicted as most likely and the MLR forecast is the category in which the continuous MLR prediction resides.

LEPS(cat)
Using LEPS(cont), S' can be integrated over category ranges to produce a scoring table to give mean values of S' for each forecast and observed category combination. For example, Table III shows the scores $(S')_{ij}$ for quint categories. Eq 21 is re-applied to provide a score for a set of forecasts, in which $(S')_p$ is now the score achieved by correct prediction of the observed category.

The assumption is that incidences of forecast-observed outcomes will be evenly distributed through each forecast-observed cell in Table III. However, in forecast sets of very high skill, outcomes may tend to be more accurate than this assumption implies, so that Table III may give lower scores than LEPS(cont). For moderate to low skill forecasts (as presently achieved in long-range forecasting), the opposite effect may apply.

A further assumption is that each forecast-observed quint outcome has the same chance probability of occurrence. If forecasts show a clear bias for certain categories (or there is clear evidence for a bias in the observed categories) we may judge that the assumption is violated and that the scoring table should be adjusted. This complication, whose principle is also applicable to LEPS(cont), is not included in this paper.

'Hits' and a discussion of applicability of Chi-squared tests
A set of forecast and observed quints can be tabulated in contingency table format (examples are shown later in Table V). A standard way of analysing association in a contingency table is to use a Chi-square test, comparing the observed frequency in each cell with that expected from chance. This is not appropriate for assessing forecasts since a) the test does not consider whether the increased frequency above chance in a particular cell is useful, b) the test does not distinguish between near misses and very bad forecasts. LEPS(cat) was designed to overcome both

Table III Scoring table for quints. The score is based on the linear error in the cumulative probability distribution, and normalised to have a chance value of zero.

		observed quint				
		1	2	3	4	5
forecast quint	1	6.4	2.7	-0.8	-3.4	-4.9
	2	2.7	2.9	0.1	-2.3	-3.4
	3	-0.8	0.1	1.4	0.1	-0.8
	4	-3.4	-2.3	0.1	2.9	2.7
	5	-4.9	-3.4	-0.8	2.7	6.4

these problems.

The proportion of correct forecasts (the 'hit rate') is a useful measure mainly because of its simplicity, but should be compared with the expected hit rate from chance. This is estimated by calculating the expected cell frequencies (as in a Chi-square test) for the cells corresponding to hits.

c) Assessing forecasts of the probability of categories.
These scores are used to assess LDA probability forecasts of each rainfall category. Skill scores for assessing probability forecasts still require further development. All scores known to the authors generally reward confident forecasts more than cautious forecasts when the score is positive, even if the confidence is not justified by the skill of the forecasts. This makes comparison of different forecast systems difficult, hence the additional discussion of probability forecasts in Section 5.2 (e).

LEPS(prob)
LEPS(cat) scores have been adapted as follows. We note the observed category (quint). Let this be quint 1 as an example. We then weight the scores S'_{i1} in Table III by the forecast probability p_i and sum over the i = 1 to 5 forecast categories:

$$S'' = \sum_i p_i S'_{i1} \qquad (22)$$

The percentage LEPS(prob) score for a set of forecasts is calculated by substituting S" for S' in the numerator of Eq 21. The denominator remains the same as that for LEPS(cat) ie Σ S" is expressed as the percentage of the score achieved by a set of

perfect categorical forecasts.

The ranked probability score (RPS)
The Ranked Probability Score (RPS, see Epstein,1969) is used here in the form recommended by Daan (1985). The score for each forecast is given by

$$RPS = 1 - \frac{\Sigma(P_i - V_i)^2}{\Sigma(C_i(1 - C_i))} \qquad (23)$$

where summation is over all categories,
P_i is the cumulative forecast probability of category i,
V_i is the cumulative observed probability of category i (0 or 1),
C_i is the cumulative climatological probability of category i
For example, $C_i = 0.4$ for quint 2, and if quint two is observed, $V_1 = 0$, $V_2 = V_3 = V_4 = V_5 = 1$

The score from chance is

$$\mu_{RPS} = \frac{\Sigma\ RPS_i}{n} \qquad (24)$$

where RPS_i is the RPS score for the forecast if category i is observed and summation is over all n possible categories (for quints, n = 5). The normalised score with a chance value of zero

is

$$RPS' = RPS - \mu_{RPS}$$

so

$$RPS\% = \frac{\Sigma(RPS')}{\Sigma(RPS'_p)} \times 100 \qquad (25)$$

where RPS'_p is the score for a categorical forecast of the observed category. As before, if the numerator is negative, the denominator should reflect the worst rather than best possible scores, and the overall percentage score is negative.

5.2 N E Brazil forecasts 1912-1985

Table IV Assessing various discriminant analysis and regression model forecasts of N E Brazil rainfall

A) Ordinary regression (and persistence for comparison)

forecast years	training period	forecasts from	model	r_f	RMS	BIAS	σ_f	LEPS% cont	LEPS% cat	Quint hit rate model	Quint hit rate chance
1949-1985	1912-48	Nov-Jan	α_t=10%	.69	52.8	+10.2	50.7	40.3	50.6	0.32	0.20
1949-1985	1912-48	Nov-Jan	a priori	.74	49.3	+8.9	52.8	45.5	52.8	0.38	0.21
1912-1948	1949-85	Nov-Jan	α_t=10%	.55	65.7	-7.3	62.6	36.1	38.0	0.40	0.23
1912-1948	1949-85	Nov-Jan	a priori	.63	58.5	-9.7	49.5	31.6	38.1	0.38	0.19
1912-1948	1949-85	Dec-Feb	a priori	.76	50.4	-12.8	59.3	46.9	51.4	0.51	0.22
1949-1985	PERSISTENCE			.24	85.1	-6.1	65.8	7.5	11.5	0.11	0.21
1913-1948	PERSISTENCE			.11	100.5	+1.8	76.5	0.1	4.2	0.19	0.26

B) Inflated regression

forecast years	training period	forecasts from	model	r_f	RMS	BIAS	σ_f	LEPS% cont	LEPS% cat	Quint hit rate model	Quint hit rate chance
1949-1985	1912-48	Nov-Jan	α_t=10%	.69	59.0	+13.3	83.4	51.6	58.4	0.40	0.20
1949-1985	1912-48	Nov-Jan	a priori	.74	58.8	+17.3	89.6	52.9	63.5	0.35	0.19
1912-1948	1949-85	Nov-Jan	α_t=10%	.55	71.0	-6.4	75.7	35.8	39.0	0.38	0.23
1912-1948	1949-85	Nov-Jan	a priori	.63	62.4	-15.0	66.5	35.4	40.7	0.50	0.22
1912-1948	1949-85	Dec-Feb	a priori	.76	56.1	-18.6	78.1	48.5	52.2	0.49	0.24

C) Discriminant Analysis

forecast years	forecasts from	model	Quint hit rate model	Quint hit rate chance	LEPS% cat	LEPS% prob	RPS%
1949-1985	Nov-Jan	a priori	0.40	0.20	54.5	36.7	33.7
1912-1948	Nov-Jan	a priori	0.38	0.17	31.1	23.1	16.4
1912-1948	Dec-Feb	a priori	0.57	0.20	53.6	32.0	26.0

Notes:
1949-1985, σ_y = 73.5; 1912-1948, σ_y = 75.6
a priori model predictors are PT1 and AT3(t). α_t = 10% indicates that model predictors were selected using 10% significance threshold. Details of the stepping process for Nov-Jan predictors:

1949-85 training period

step	variable entered	F-to-enter	sig
1	AT3(t)	22.9	1%
2	PT1	11.9	1%
3	AT6(t)	5.6	2.5%
4	PT3	3.5	10%
5	AT5	2.9	10%

1912-48 training period

step	variable entered	F-to-enter	sig
1	AT3(t)	15.5	1%
2	PT1	5.3	5%
3	PT6	3.5	10%

For details of skill scores see section 5.1

Table IV assesses forecasts for 1949-1985 (1912-1948) that are made using models with a 1912-48 (1949-1985) training period. SST data for the early part of the century are therefore important so seasonal values of the EC time series are used to minimise noise. In the real-time predictions discussed in section 5.3, a final forecast from monthly February EC time series values is also made since Fig 10 suggested that, for the El Nino EC time series, values closest to the N Nordeste rainfall season provide the best predictor.

a) Ordinary regression results

Models which comprise AT3(t) and PT1 are referred to as the 'a priori' models. Using Nov-Jan predictors these correspond to MLR models selected by a threshold significance level of 5% in 1912-1948 and 1% in 1949-1985 (see stepping details at the bottom of Table IV). Results from models selected using a 10% significance threshold are presented for comparison. The 'a priori' models generally perform best on all skill measures, suggesting that the stepwise method is not adding useful predictors to AT3(t) and PT1. All models shown perform much better than persistence on all measures except BIAS. However, the model BIAS values are generally only one standard error from 0, so are not statistically significant and probably arise due to sampling variation.

When we forecast for the years 1912-1948, the results from Nov-Jan predictors are good, but can be improved to those achieved for 1949-1985 by using Dec-Feb predictors. It has not yet been possible to deduce if this is due to less reliable SST data or a change in the lead time of SSTs on N Nordeste rainfall in the earlier years.

b) Comparison of inflated and ordinary MLR

RMS is larger for inflated MLR forecasts, because the standard deviation of the forecasts (σ_f) has been raised close to that of the standard deviation of the observed (σ_v), while the correlation (r_f) remains constant. The LEPS scores for the inflated forecasts are however generally better. Inflated regression forecasts may be best in those applications when forecast utility measures are closer to LEPS than RMS. The higher BIAS values for inflated forecasts are still only about one standard error from 0 because σ_f has been raised.

c) Comparison of LDA and MLR forecasts

LDA and ordinary MLR forecasts have very similar LEPS(cat) scores. The mean ratio of model hit rate to chance hit rate in Table IVC is 2.34, compared to 2.05 and 2.06 for the same ordinary and inflated MLR forecast sets, so LDA does best with a hit rate well over twice that expected from chance. RPS and LEPS(prob) show considerable agreement despite their very different formulation, but these and other probability forecast scores require further study and comparison to increase their utility. Probability forecasts are returned to in e) below.

d) Comparisons with other studies

The correlation between forecast and observed (r_f) can be directly compared with other prediction studies for seasonal rainfall in the tropics. Values over 0.7 have rarely been achieved over such a long testing period. Typical results include $r_f = 0.7$ for predictions of N Australian seasonal rainfall 1951-1980 (Nicholls, 1984), $r_f = 0.4$ to 0.5 for predictions of coastal Kenya seasonal rainfall (Farmer, 1988), $r_f = 0.55$ for Java

seasonal rainfall (Hastenrath, 1987). Recently, very large values of r_f have been reported (>0.8) for prediction experiments for all India summer rainfall (Shukla and Mooley, 1987) but Hastenrath (1988) has shown that these results for the short period 1969-1985 deteriorate when the testing period is extended to 1959-1985 (r_f = 0.75), either due to sampling variability or a real fluctuation in the predictability of the Indian monsoon. For NE Brazil, HWC (1984) using predictor data for January achieved r_f = 0.64 with their March-April rainfall series and r_f = 0.68 with their March-September series. The testing period was 1958-1972, so our results using AT3(t) and PT1 for 1949-1985 (r_f = 0.74) correspond to a useful advance in terms of the longer period and hence greater confidence in the results and in the slight improvement in r_f.

A useful advance on the results of HWC (1984) is also found in our BIAS values. HWC's forecasts for 1958-72 tended to be much too dry; analysis of their results suggests the BIAS is about three standard errors from zero, which is statistically significant at the 1% level. This may have been due to spurious trends that are now believed to be present in surface wind data acquired from ship reports (Cardone et al, in press).

e) Further analysis of quint forecasts

Table V contains contingency tables of forecast and observed quint for some of the forecast sets in Table IV. The improvement in quint 1 forecasts for 1949-85 in Table VB illustrates the potential benefits to be gained from inflated regression.

The range (quint) in which the continuous MLR prediction resided was, for Table 5, taken to be the predicted range; this is the usual way in which continuous predictions are converted to predictions of ranges (eg Folland et al, 1986). However, the probability of different ranges can be estimated if the distribution of the expected prediction error is known. Making the assumptions of MLR, the error distribution is approximately normal with a standard deviation equal to the SE of the prediction (Eq 8). From this, the ordinary MLR forecasts in Table V have been converted to probability forecasts of quints. Table VI presents the mean forecast probabilities for those forecasts when the continuous prediction resided in a) an extreme quint, b) quint 2 or 4, and c) quint 3. For these 3 subsets of the forecasts, the proportion of years observed to be in each category is also presented. If the probability of each quint has been accurately forecast, the mean forecast probabilities and the observed proportions should be similar. For extreme quint forecasts, the mean probability forecast is good; just a little too confident. For quint 3 forecasts the mean forecast probability of each quint correctly expects there to be least

Table V Contingency tables of forecast quint v observed quint for some of the sets of forecasts in Table IV: A = ordinary regression, B = inflated regression, C = discriminant analysis.

		1949-1985 forecasts					1912-1948 forecasts					
A)		observed						observed				
		Q1	Q2	Q3	Q4	Q5		Q1	Q2	Q3	Q4	Q5
f	Q1	0	2	0	1	0	f Q1	9	1	2	0	2
r	Q2	5	3	1	0	0	r Q2	2	1	0	0	1
c	Q3	1	2	2	1	1	c Q3	1	0	2	1	2
s	Q4	0	2	4	4	0	s Q4	0	1	2	3	2
t	Q5	0	0	0	3	5	t Q5	0	0	1	0	4
B)		observed						observed				
		Q1	Q2	Q3	Q4	Q5		Q1	Q2	Q3	Q4	Q5
f	Q1	4	4	1	1	0	f Q1	9	2	2	0	2
r	Q2	2	1	1	0	0	r Q2	3	0	0	0	1
c	Q3	0	2	1	1	0	c Q3	0	0	2	0	2
s	Q4	0	0	2	2	1	s Q4	0	1	0	3	1
t	Q5	0	2	2	5	5	t Q5	0	0	3	1	5
C)		observed						observed				
		Q1	Q2	Q3	Q4	Q5		Q1	Q2	Q3	Q4	Q5
f	Q1	1	1	1	0	0	f Q1	9	0	1	0	1
r	Q2	4	4	1	1	0	r Q2	3	2	0	0	3
c	Q3	0	1	0	0	0	c Q3	0	0	3	0	1
s	Q4	1	1	3	4	0	s Q4	0	1	2	4	3
t	Q5	0	2	2	4	6	t Q5	0	0	1	0	3

Notes:
Results are for 'a priori' models shown in Table IV.
1912-1948 forecasts are from Dec-Feb predictor values, 1949-1985 are from Nov-Jan predictor values.

skill in this subset of forecasts. Least skill in long-range forecasts of near normal is often found and is an active area of debate (eg see Toth, 1989).

Given the SE of these forecasts and the narrowness of quints 2 and 4, a prediction residing in quint 2 or 4 always implies that the extreme quint is most likely to occur, and this is reflected in the mean forecast probabilities (0.20 for the quint in which the forecast resides, 0.41 for the adjacent extreme quint). However, the hit rate of the quint 2/4 forecasts is rather better than predicted (0.35 correct, only 0.29 observed in the adjacent extreme). The main reason for this is that the conversion to probability forecasts does not expect the RMS error of quint 2/4 forecasts to be less than the RMS on other forecasts (see Table VI). The difference between the RMS errors in Table VIA are not quite statistically significant at the 10% level, so their effects on the observed probability distributions may be fortuitous.

Table VI Analysis of the ordinary MLR and LDA forecasts in Table V in terms of the probability forecast for each quint. The forecasts have been sub-divided by the forecast quint shown in Table V.

A) Mean quint probabilities and observed proportions of each quint for subsets of MLR continous forecasts.

Subset 1: Continuous MLR prediction resides in an extreme quint (30 forecasts).
RMS error for continuous predictions is 54.0

	forecast quint	1 quint in error	2 quints in error	3 quints in error	4 quints in error
forecast probability	0.69	0.13	0.11	0.04	0.02
observed proportion	0.60	0.20	0.10	0.03	0.07

Subset 2: Continuous MLR prediction resides in quint 2 or 4 (31 forecasts).
RMS error for continuous predictions is 44.3

	forecast quint	adjacent extreme	quint 3	2 quints in error	3 quints in error
forecast probability	0.20	0.41	0.20	0.10	0.08
observed proportion	0.35	0.29	0.22	0.10	0.03

Subset 3: Continuous MLR prediction resides in quint 3 (13 forecasts).
RMS error for continuous predictions is 52.7

	forecast quint	1 quint in error	2 quints in error
forecast probability	0.24	0.17	0.21
observed proportion	0.31	0.15	0.19

B) Mean quint probabilities and observed proportion of each quint for subsets of LDA predictions.

Subset 1: Extreme quint forecast as most likely (32 forecasts).

	forecast quint	1 quint in error	2 quints in error	3 quints in error	4 quints in error
forecast probability	0.53	0.22	0.15	0.06	0.04
observed proportion	0.59	0.16	0.16	0.06	0.03

Subset 2: Quint 2 or 4 forecast as most likely (37 forecasts).

	forecast quint	adjacent extreme	quint 3	2 quints in error	3 quints in error
forecast probability	0.36	0.23	0.23	0.12	0.06
observed proportion	0.38	0.27	0.16	0.08	0.11

Subset 3: Quint 3 forecast as most likely (5 forecasts).

	forecast quint	1 quint in error	2 quints in error
forecast probability	0.33	0.23	0.10
observed proportion	0.60	0.10	0.10

A similar analysis of quint probabilities was performed on the LDA forecasts in Table V. The mean forecast probabilities (Table VIB) are more accurate than those of MLR in the subset of extreme forecasts and especially in the subset of quint 2/4 forecasts. Again the highest hit rate is expected for extreme forecasts and the lowest for average forecasts, though the small number of average forecasts makes their assessment difficult.

f) The forecasts by year 1912-1985

The forecasts in Tables VA and VC are plotted by year in Fig 14. There is close agreement between the most likely quint forecast by LDA and the quint in which the continuous MLR prediction resides. Particularly noteworthy is the ability of the systems to forecast the onset, persistence and breakdown of the runs of very dry years 1914-15, 1930-32 and 1941-43.

Despite the strong El Nino in 1983 (PT1 predictor in Nov-Jan = 8.8), LDA does not forecast quint 1 as most likely because of the large negative values of AT3(t) (= -0.9). Quint 2 is forecast as most likely (p = 0.42), followed by quints 1 (p = 0.34) and 5 (p = 0.10), introducing some bimodality. MLR can only produce a unimodal forecast; not surprisingly a near average forecast results. This illustrates a potential benefit of LDA. The most severe drought in the last 20 years occurred in 1983 (Rao et al 1986). Models which use March-May values of our two predictors do correctly indicate the drought, since AT3(t) changed rapidly from negative values to positive values (+1.05 in March-May), a change that is consistent with the relationship between Atlantic SST and El Nino identified in Ward et al (1988). A link between ENSO and the ocean-atmosphere system in the tropical Atlantic is also discussed by Wolter (1987) and inclusion of an interaction between our two predictors in the forecast models requires further consideration.

5.3 Experimental forecasts produced in real-time 1987-1989

SSTAs are today available in near real-time, so it is possible to prepare forecasts before the main N Nordeste rainfall season. Experimental forecasts were prepared in each year 1987 to 1989 using Nov-Jan values of SSTA EC predictors and February values of the predictors. The forecasts were distributed in early March to a small number of scientists. Table VII shows the LDA probability forecasts made from February SSTA EC time series values for quints of the Quixeramobim/Fortaleza (QF) March-May index used in Ward et al (1988). Forecasts with similar probability distributions were also made for HWC's March-April index and Nobre's Feb-May index (since 1988), but these series have not been updated so the forecasts cannot yet be properly verified.

A forecast of quint 1 (very dry) was made for 1987 and the rainfall season, after a very wet March, was dominated by two very dry months; the QF standardised anomaly is just sufficiently negative to score 1987 as one of the driest 20% of years (ie

Table VII NE Brazil seasonal forecasts 1987-1989 that were produced in real-time using the LDA technique and their preliminary verification.

A) Forecast probabilities for quints of March to May Quixeramobim/Fortaleza index.

	forecast probability of quint				
	Q1	Q2	Q3	Q4	Q5
1987	.45	.18	.14	.18	.05
1988	.03	.07	.08	.31	.51
1989	.00	.08	.06	.18	.68

B) Data for March-May Quixeramobim/Fortaleza (QF) index 1987-1989

	Quixeramobim				:	Fortaleza				:	combined QF index	
	March	April	May	SU	:	March	April	May	SU	:	SU	quint
mean	166	160	115		:	304	246	193		:		
1987	235+	61	20	-68	:	414+	178	40	-75	:	-72	Q1
1988	140	192	163	+21	:	562	287	306	+97	:	+59	Q4
1989	180	305	309	+171	:	287	310	188	-25	:	+73	Q5

SU = March-May rainfall anomaly in station standard deviations x 100
Combined QF index quint boundaries for 1951-80 are -70.1, -16.1, 15.1, 67.5
Data are from CLIMAT reports except + which are from a bulletin by FUNCEME, Ceara State, Brazil (whose Fortaleza site is slightly different)

quint 1) using 1951-80 as the base period. For 1988, forecasts from Nov-Jan predictors were contradictory, but by February the 1987 El Nino event had decayed sufficiently to allow the value of AT3(t) to influence the forecast most and produce a clear prediction of the wet (p = 0.31) or very wet (p = 0.51) quint. After a dry start, the 1988 rainfall season was well above average, categorised as quint 4 (wet) in the QF index. In 1989, a combination of large negative values for AT3(t) and PT1 produced a confident prediction of very wet conditions. This confidence was not fully reflected in the released forecast because the complete AT3 predictor (including the extra-tropics) did not suggest such wet conditions and SSTAs associated with La Nina were decaying quite quickly. Like 1988, the season started dry, but at Quixeramobim became extremely wet in late March, April and early May, ensuring a quint 5 season on the QF index. Analysis of Monitor Climatico (produced by FUNCEME, Ceara State Met. Office, Fortaleza) and outgoing long-wave radiation patterns suggest that Nobre's and HWC's indices will be a little higher in 1987 than the QF index, but similar in 1988 and 1989.

Overall, the three experimental forecasts that were produced in real-time and disseminated have shown good skill.

6. Conclusions

Statistical methods to predict seasonal rainfall in NE Brazil have been developed. Measures of sea surface temperature were used as predictors because GCM integrations have shown that physical mechanisms exist to link SST to NE Brazil rainfall and because a carefully quality controlled dataset of SST is available.

A covariance eigenvector analysis of SSTAs in the Atlantic and Pacific oceans identified several patterns of SSTA variability. Two of the patterns showed a strong relationship with seasonal rainfall in N Nordeste; one in the tropical Atlantic which is similar to that previously discussed by Hastenrath and Heller (1977) and one representing ENSO in the Pacific which was previously discussed in relation to NE Brazil rainfall by Covey and Hastenrath (1978). Pre-rainfall season values of the time series of these two patterns provide the most powerful SST predictors of seasonal NE Brazil rainfall yet discovered. Test forecasts over many years suggest that at a lead time of a month or so, about half of the interannual variability of seasonal N Nordeste rainfall is predictable from these two patterns. By using a variety of assessment methods, many different attributes of the forecasts were revealed. At a lead time of six months, the tropical Atlantic SSTA predictor still shows a statistically significant correlation with NE Brazil rainfall, but the level of correlation would yield a very low level of forecast skill.

Two statistical forecast techniques have been considered. The MLR method is relatively simple. Inflated regression was shown to be a potentially useful way of overcoming the low variance in MLR predictions, though conversion to a probability forecast also enables extreme events to be expected with realistic frequency. LDA is a step towards techniques that specifically estimate the probability distribution of possible outcomes. It allows some non-linearity in the predictor-predictand relationships and allows bi-modal forecasts. In this application, LDA's probability forecasts indicate best the likelihood of each category's occurrence. LDA is however not ideal and more efficient techniques may be found in the future. Objective methods for selecting the predictors for the forecast models have been briefly considered. The view taken here is that they should be used along with physical understanding, GCM experiments and extensive empirical studies.

This paper has built on previous work, and developed methods that are now being used to produce successful experimental forecasts of NE Brazil seasonal rainfall in real-time. However, there is scope for much development. Improved analysis of the SSTA data, including rotation of the eigenvectors, should better define the important predictor SSTA paterns. Other predictors, such as monthly or seasonal indices of atmospheric circulation similar to those used by HWC (1984), may combine with the SSTA predictors to increase skill since the set of predictors would then provide a more complete summary of the state of the pre-rainfall season ocean-atmosphere system. The main hindrance is the uncertain quality of the atmospheric circulation data, and improvements to the data may be needed first.

Prediction using a GCM forced with the pattern of observed SSTAs prior to the rainfall season could be attempted (as done for the Sahel in Owen and Ward, 1989). GCM integrations are already leading to better understanding of the links between SSTs and atmospheric circulation in the vicinity of the N Nordeste

(Mechoso and Lyons, 1988). Our empirical results suggest that it is important to address the reasons for the links between NE Brazil rainfall and SSTAs over the whole globe including the Indian Ocean.

APPENDIX I

Presentation of results in this paper is simplified by presenting and using only one set of Atlantic and one set of Pacific eigenvectors. The choice of using all seasons eigenvectors for the Atlantic and seasonally specific eigenvectors for the Pacific was based on the desire to produce the clearest versions of the patterns in Figs 8a and 9a. For the Pacific, clear El Nino eigenvectors result from analysis of any of the four seasons; Dec-Feb patterns are presented since this is the period from which forecasts are made, but results are not sensitive to this choice.

APPENDIX II

The LEPS skill score is
$S = 1 - \mathrm{mod}(p_f - p_v)$
where p_f and p_v are the cumulative probabilities of the forecast and observed (eg see Fig 13). The expected value of the score S when a particular combination of p_v and p_f occurs is given by a standard statistical result as

$$\mu_s = \frac{\int_{p_f=0}^{p_f=1} S dp_f \int_{p_v=0}^{p_v=1} S dp_v}{\int_{p_v=0}^{p_v=1}\int_{p_f=0}^{p_f=1} S dp_f dp_v} \qquad \text{(A1)}$$

now

$$\int_{p_f=0}^{p_f=1} S dp_f = \int_{p_f=0}^{p_f=1} 1 - \mathrm{mod}(p_v - p_f)\, dp_f$$

$$= \int_{p_f=0}^{p_f=p_v} 1 - (p_f - p_v)\, dp_f + \int_{p_f=p_v}^{p_f=1} 1 - (p_v - p_f)\, dp_f \qquad \text{(A2)}$$

evaluating this and the other integrals yields

$$\mu_s = 1.5(p_f - (p_f)^2 + 0.5)(p_v - (p_v)^2 + 0.5)$$

Acknowledgements

We must thank Stuart Brooks for his help in the early stages of this work, David Parker and Gil Ross for their helpful comments, and Andrew Colman for his help with the programming. We are indebted to Carlos Nobre (Instituto de Pesquisas Espaciais -INPE, Brazil) and Stefan Hastenrath (University of Wisconsin) for the provision of standardised rainfall series.

References

Afifi, A.A. and Azen, S.P. 1979. Statistical analysis - a computer orientated approach, Academic Press, New York.

Bhalme, H.N., Jadhav, S.K., Mooley, D.A. and Ramana Murty, Bh.V. 1986. 'Forecasting of monsoon performance over India', J.Climatol., 6, 347-354.

Bhalme, H.N., Rahalkar, S.S. and Sikder, A.B. 1987. 'Tropical quasi-biennial oscillation of the 10-mb wind and Indian monsoon rainfall - implications for forecasting', J. Climatol., 7, 345-353.

Bottomley, M., Folland, C.K., Hsiung, J., Newell, R.E. and Parker, D.E. 1989. Global ocean surface temperature atlas. A joint project by the Meteorological Office and Massachusetts Institute of Technology. MIT Press, in press.

Burden,R.L. and Faires,J.D. 1985. Numerical Analysis, Prindle, Weber and Schmidt, Boston.

Cardone, V.J., Greenwood, J.G. and Cane, M.A. 'On trends in historical marine wind data', J. Clim., in press.

Caviedes,C.N. 1973. 'Secas and El Nino: two simultaneous climatological hazards in South America', Proc. Amer. Geogr., 5, 44-49.

Chung, J.C. 1982. 'Correlations between the tropical Atlantic trade winds and precipitation in NE Brazil',J. Climatol., 2, 35-46.

Covey, D.C. and Hastenrath, S. 1978. 'The Pacific El Nino phenomenon and the Atlantic circulation', Mon. Weath. Rev., 106, 1280-1287.

Daan, H. 1984. Scoring rules in forecast verification. WMO short- and medium-range weather prediction research publication series No. 4, pp62.

Daan, H. 1985. 'Sensitivity of verification scores to the classification of the predictand'. Mon. Wea. Rev., 113, 1384-1392.

Epstein, E.S. 1969. 'A scoring system for probability forecasts of ranked categories', J. Appl. Met., 8, 985-987.

Farmer, G. 1988. 'Prediction of coastal Kenya seasonal rainfall', J. Climatol., 8, 489-497.

Folland, C.K. and Colman, A. 1988. An interim analysis of the leading covariance eigenvectors of worldwide sea surface temperature anomalies for 1901-1980. Long Range Forecasting and Climate Memorandum No 20 (unpublished). Available from the Meteorological Office.

Folland, C.K., Palmer, T.N. and Parker, D.E. 1986. 'Sahel rainfall and worldwide sea temperatures', 1901-1985, Nature, 320, 602-607.

Folland, C.K. and Owen, J.A. 1988. 'GCM simulation and prediction of Sahel rainfall using global and regional sea surface temperatures', In: WMO Working Group on Numerical Experimentation Workshop on GCM comparison, ECMWF, Reading, 11-13 May 1988 (in press).

Folland, C.K., Woodcock, A. and Varah, L. 1986. 'Experimental monthly long-range forecasts for the United Kingdom. Part III Skill of the monthly forecasts'. Met. Mag., 115, 377-395.

Gill, A.E. and Rasmusson, E.M. 1983. 'The 1982-83 climate anomaly in the equatorial Pacific, Nature 306, 229-234.

Hastenrath, S. and Heller, L. 1977. 'Dynamics of climatic hazards in Northeast Brazil', Q.J.R. Met. Soc., 103, 77-92.

Hastenrath, S., Wu, M.-C. and Chu, P.-S. 1984. 'Towards the monitoring and prediction of Northeast Brazil droughts', Q.J.R.Met. Soc., 110, 411-425.

Hastenrath, S. 1987. 'Predictability of Java monsoon rainfall anomalies: a case study', J. Clim. Appl. Met., 26, 133-141.

Hastenrath, S. 1988. 'Prediction of Indian monsoon rainfall: Further exploration',J.Clim., 1, 298-304.

Jolliffe, I.T. 1986. Principal Component Analysis, Springer series in statistics, Springer-Verlag.

Kane, R.P. and Trivedi, N.B. 1988. 'Spectral characteristics of the annual rainfall series for northeast Brazil', Clim. Change, 3, 317-336.

Katz, R.W. 1987 'Use of cross correlations in the search for teleconnections', J. Climatol., 8, 242-253.

Krishnamurti, T.N., Kumar, A. and Li, X. 1987. 'Results of extensive integrations with simple NWP models over the tropics during FGGE', Tellus, 39A, 152-160.

Labitzke, K. and van Loon, H. 1988. 'Associations between the 11-year solar cycle, the QBO and the atmosphere. Part II: Surface and 700mb in the Northern hemisphere winter', J. Climate, 1, 905-920.

Lau, N.-C. 1985. 'Modelling the seasonal dependence of the atmospheric response to observed El Ninos in 1962-76', Mon. Weath. Rev., 113, 1970-1996.

Lamb, P.J., Peppler, R.A. and Hastenrath, S. 1986. 'Interannual variability in the tropical Atlantic', Nature, 322, 238-240.

Lindley, D.V. 1965. Introduction to probability and statistics from a Bayesian viewpoint Part 2: Inference, Cambridge University Press, 211.

Livezey, R.E. and Chen, W.Y. 1983. 'Statistical field significance and its determination by Monte Carlo techniques', Mon. Weath. Rev., 111, 46-59.

Markham C. and McLain D. 1977. 'Sea surface temperature related to rain in Ceara, Northeast Brazil', Nature, 265, 320-323.

Maryon, R.H., and Storey, A.M. 1985. 'A multivariate statistical model for forecasting anomalies of half-monthly mean surface pressure', J. Climatol., 5, 561-578.

Mechoso, C.R. and Lyons, S.W. 1988. 'On the atmospheric response to SST anomalies associated with the Atlantic warm event during 1984', J. Clim., 1, 422-428.

Moura, A.D. and Shukla, J. 1981. 'On the dynamics of drought in Northeast Brazil. Observations, theory and numerical experiments with a general circulation model', J. Atmos. Sci., 38, 2653-2675.

Namias, J. 1972. 'Influence of northern hemisphere general circulation on drought in Northeast Brazil', Tellus, 24, 336-343.

Nicholls, N. 1984. 'The stability of empirical long-range forecast techniques: a case study', J. Clim. Appl. Met., 23, 143-147.

Nicholls, N., 1987. 'Prospects for drought prediction in Australia and Indonesia', in Wilhite, D.A. et al (Ed) Planning for drought, Westview Press, Boulder and London, 61-67.

North, G.R., Bell, T.L., Cahalan, R.F. and Moeng, F.J. 1982. 'Sampling errors in the estimation of Empirical Orthogonal Functions', Mon. Wea. Rev., 110, 699-706.

Owen, J.A. and Ward, M.N. 1989. 'Forecasting Sahel rainfall', Weather, 44, 57-64.

Parker, D.E. and Folland, C.K. 1988. 'The Meteorological Office Historical Sea Surface Temperature Dataset', In: Recent Climatic Change - a regional approach. Ed S. Gregory, Belhaven Press, 41-50.

Parker, D.E., Folland, C.K. and Ward, M.N. 1988. Sea surface temperature anomaly patterns and prediction of seasonal rainfall in the Sahel region of Africa, Ibid, 166-178

Parker, D.E. and Folland, C.K. 'Worldwide surface temperature trends since the mid-19th Century', In: Proc. U.S D.o.E Workshop on Greenhouse-Gas-Induced Climatic Change, Amherst, Mass., 8-21 May 1989, Elsevier (in press).

Rao, V.B., Satyamurty, P., Ivaldo, J., and de Brito, B. 1986. 'On the 1983 drought in Northeast Brazil', J.Climatol., 6, 43-51.

Richman, M.B. 1986. 'Rotation of principal components', J.Climatol., 6, 293-335.

Rogers, J.C. 1985. 'Atmospheric circulation changes associated with the warming in the N Atlantic in the 1920's', J. Clim. Appl. Met., 24, 1303-1310.

Shukla, J. and Fennessy, M.J. 1988. 'Prediction of time-mean atmospheric circulation and rainfall: Influence of Pacific sea surface temperature anomaly', J. Atmos. Sci., 45, 9-28.

Shukla, J. and Mooley, D.A. 1987. 'Empirical prediction of the summer monsoon rainfall over India', Mon. Weath. Rev., 115, 695-703.

Toth, Z., 1989. 'Dependency of long-range temperature predictability in Hungary on circulation weather type and forecast category' In: Proceedings 13th Annual Climate Diagnostics Workshop, Oct 31 - Nov 4, 1988, 497-499.

Ward, M.N., Brooks, S. and Folland, C.K. 1988. 'Predictability of seasonal rainfall in the N Nordeste region of Brazil', in Gregory, S. (Ed) Recent climate change, Belhaven, London, 237-251.

Weisberg, S. 1976. Applied linear regression, Wiley series in probability and statistics, New York.

Wolter, K. 1987. 'The Southern Oscillation in surface circulation and climate over the Tropical Atlantic, Eastern Pacific and Indian Oceans as captured by cluster analysis', J. Clim. Appl. Met., 26, 540-558.

Figure headings

Figure 1. Location map of N Nordeste. The rainfall series of Nobre is based on stations throughout N Nordeste. The series of HWC(1984) used stations from within the area marked by the dashed line.

Figure 2. Standardised seasonal anomaly rainfall series for the N Nordeste. Values are x100. 1912-1981 for February-May from Nobre (INPE, personal communication). 1982-1985 are updates of the HWC(1984) March-April series (Lamb, Peppler and Hastenrath (1986), and Hastenrath, personal communication)

Figure 3. Correlations for 1901-1980 (in hundredths) between seasonal SSTA in the shaded square and SSTA in surrounding squares (from Morgan, personal communication).

Figure 4. Number of seasons with sufficient sea surface temperature ship observations to allow estimation of the season's anomaly.

Figure 5a Correlations (in hundredths) between SSTA in March-May and N Nordeste rainfall index 1912-1985. Correlations significant at the 95% level are shaded.

Figure 5b. As Figure 5a but for 1949-1985.

Figure 5c. As figure 5a but for 1912-1948.

Figure 6a. First covariance eigenvector of seasonal SSTAs in the Atlantic ocean (all seasons included) 1901-1980. Values are x1000.

Figure 6b. Time series for Atlantic eigenvector 1.

Figure 7. Second Atlantic eigenvector.

Figure 8a. Third Atlantic eigenvector.

Figure 8b. March-May values of the Atlantic eigenvector 3 time series (AT3, solid line) along with N Nordeste rainfall index (dashed line).

Figure 9a. First covariance eigenvector of seasonal Dec-Feb SSTAs in the Pacific ocean 1901-1980.

Figure 9b. March-May values of time series for eigenvector in Fig 8a (PT1, solid line) along with N Nordeste rainfall (dashed line).

Figure 10. Correlations 1912-1985 between SSTA eigenvector time series and N Nordeste rainfall. JA = July-August values of eigenvector time series, AS = August-September, SO = Sept-Oct etc. In the plot, A = correlations with Atlantic eigenvector 3 time series, P = correlations with Pacific eigenvector 1 time series.

Figure 11. As Figure 9, but N = correlations with series AT3(ne), ie using Atlantic data north of 40N, T = correlations with series AT3(t), ie using tropical Atlantic data (see text).

Figure 12 Probability density functions for value of AT3(t) (Atlantic eigenvector 3 time series, tropical signal) in December-February. Function $f_i(x)$ is for years when quint i was observed in N Nordeste 1912-1981.
If AT3(t) = -0.9 (marked above with a vertical dashed line):
$f_1(x)=0.01$, $f_2(x)=0.09$, $f_3(x)=0.08$, $f_4(x)=0.18$, $f_5(x)=0.38$
so (from equation 12) the forecast probability of each quint is:
$Pr(Q_1)=0.01$, $Pr(Q_2)=0.12$, $Pr(Q_3)=0.11$, $Pr(Q_4)=0.24$, $Pr(Q_5)=0.51$

Figure 13 Cumulative probability distribution of the NE Brazil standardised rainfall series. For the forecast f shown, the cumulative probability is $p_f = 0.39$, and for the observed v, the cumulative probability is $p_v = 0.19$.

Figure 14 LDA and ordinary MLR forecasts in Table V plotted as time series along with the observed quint.

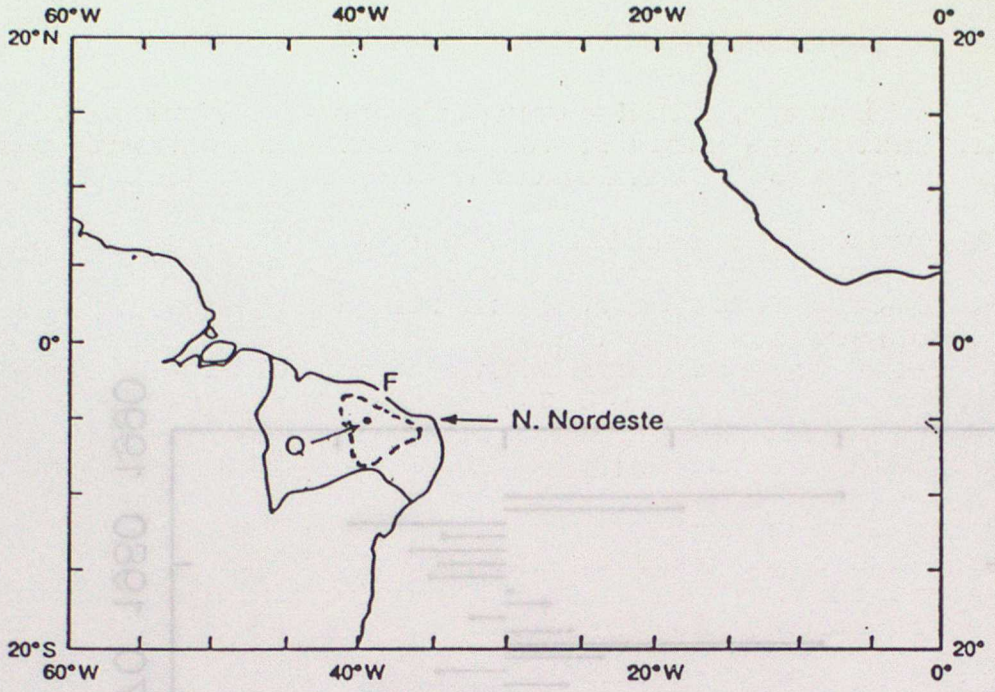

Key:

Q Quixeramobim
F Fortaleza

Figure 1

Figure 2.

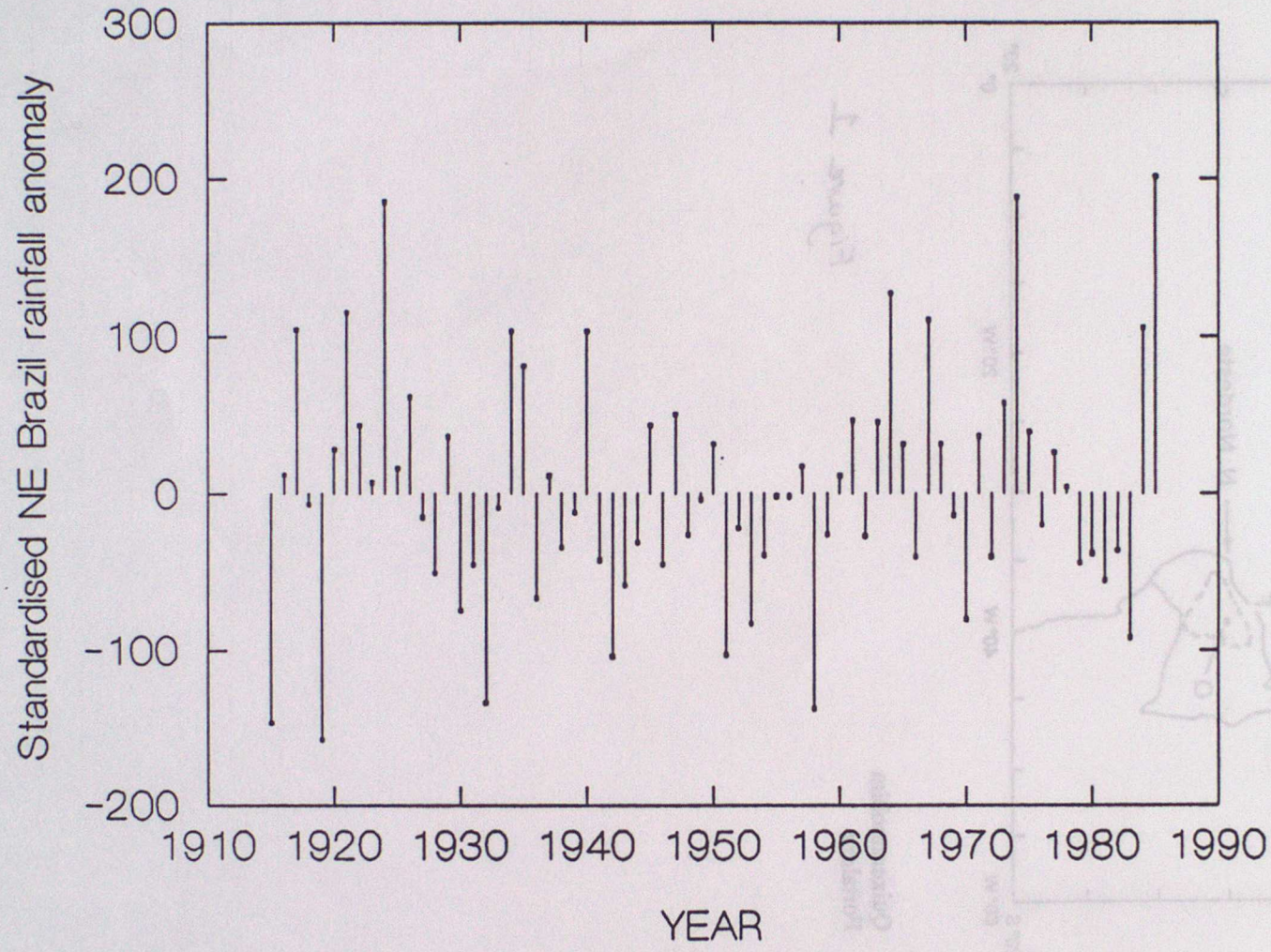
Standardised NE Brazil rainfall anomaly
300
200
100
0
-100
-200
1910
1920
1930
1940
1950
1960
1970
1980
1990
YEAR

Figure 3.

CORRELATION FUNCTIONS FOR SHADED SQUARES

ALL VALUES MULTIPLIED BY 100

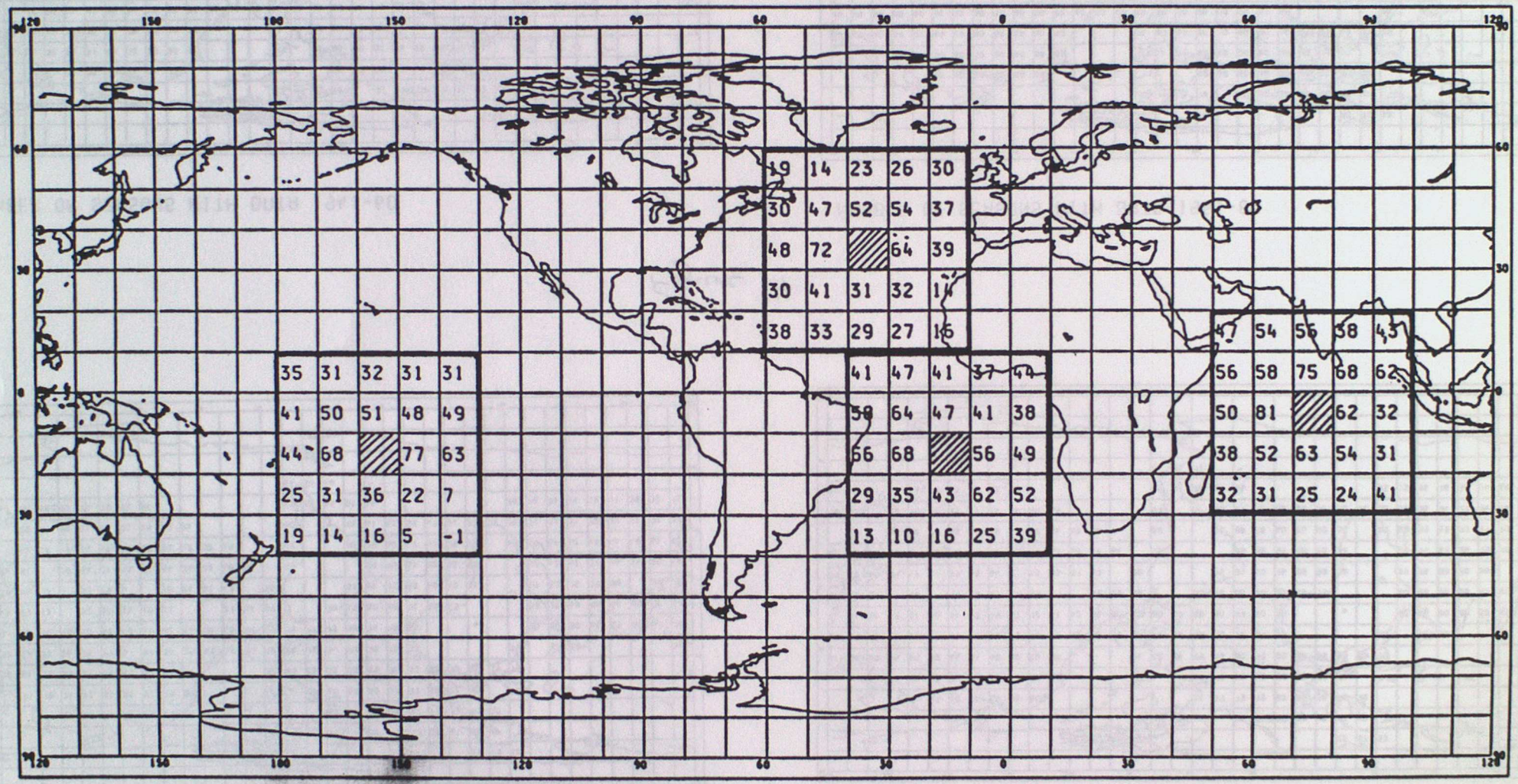

NUMBER OF SEASONS WITH DATA 1901-20

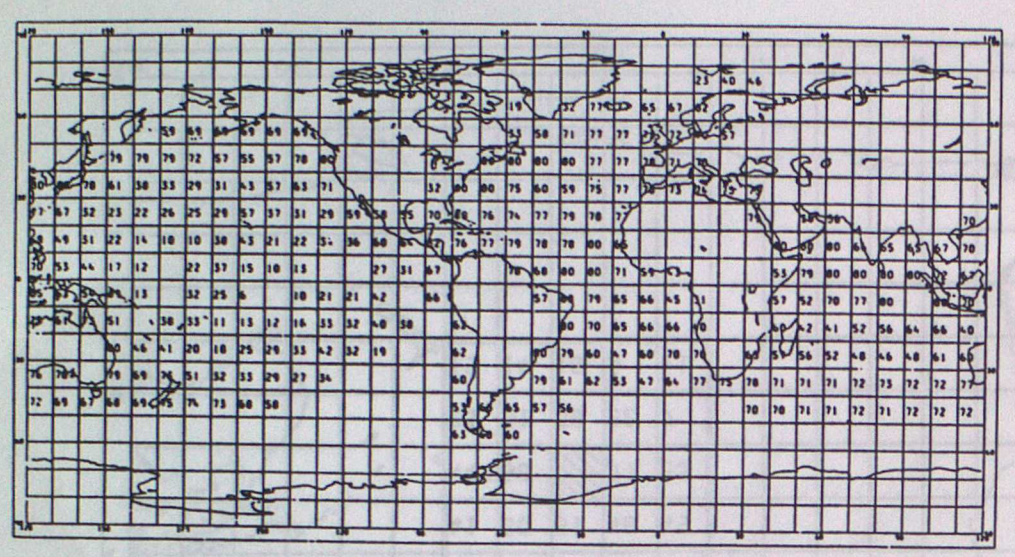

NUMBER OF SEASONS WITH DATA 1921-40

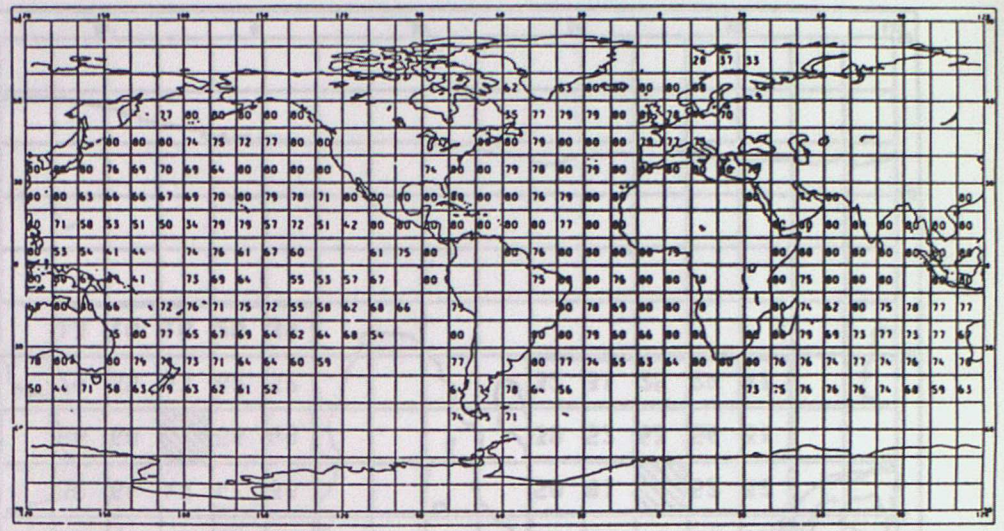

Figure 4.

NUMBER OF SEASONS WITH DATA 1941-60

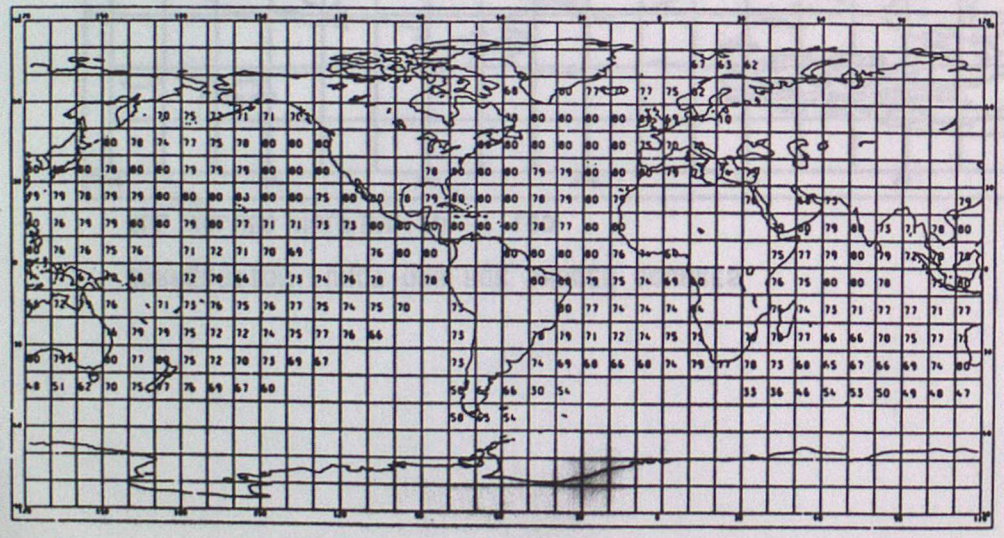

NUMBER OF SEASONS WITH DATA 1961-80

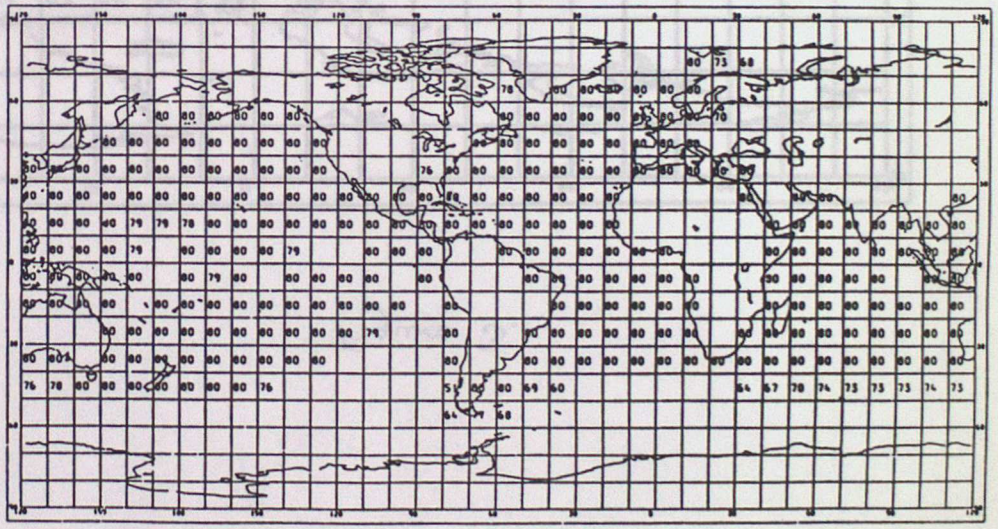

Figure 5a.

PERIOD = 1912 TO 1985 . SEASON IS NUMBER 1 MAR-MAY

NO INSTRUMENTAL CORRECTIONS TO SST

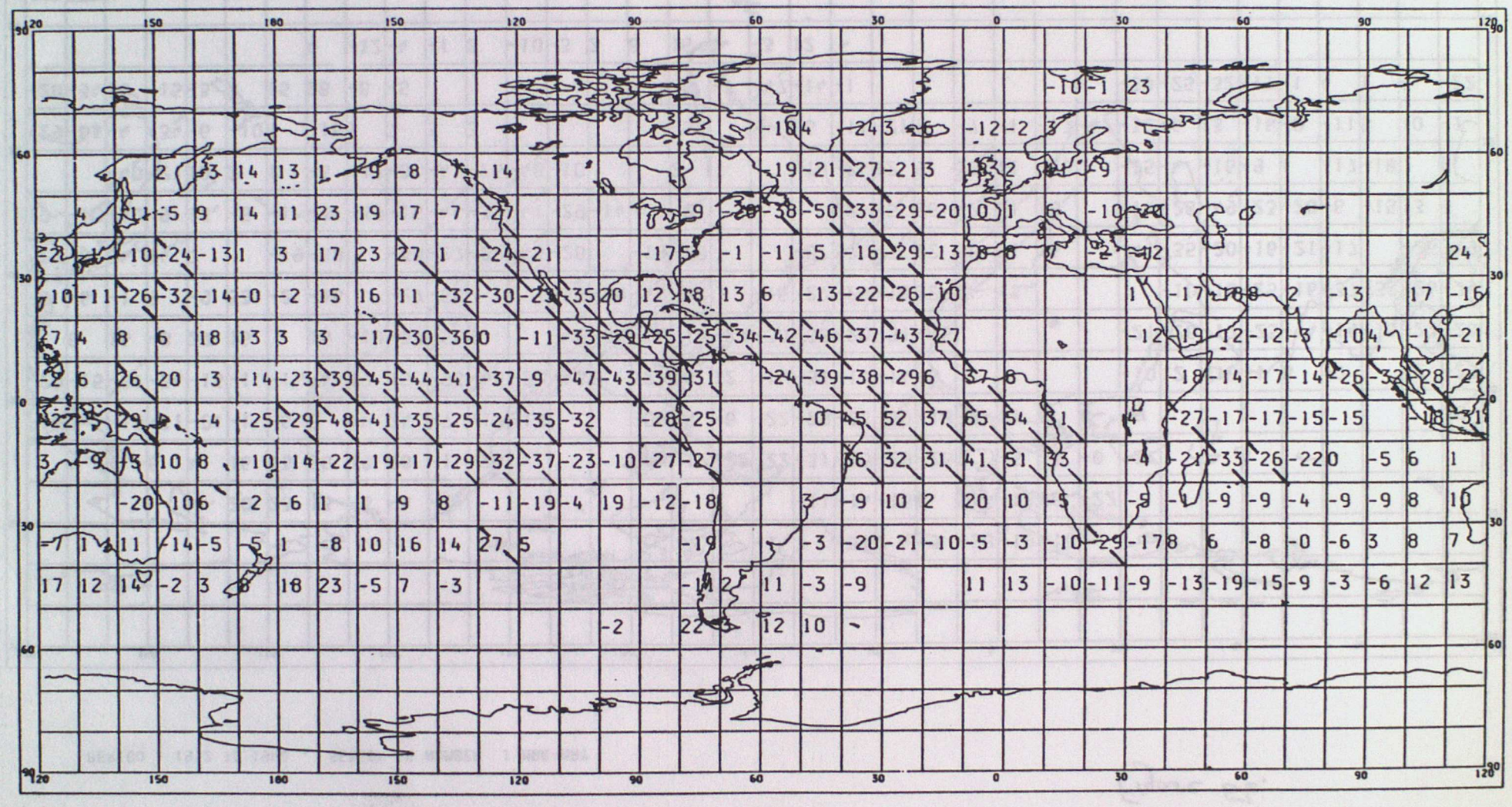

Figure 5b.

PERIOD = 1912 TO 1948 . SEASON IS NUMBER 1 MAR-MAY

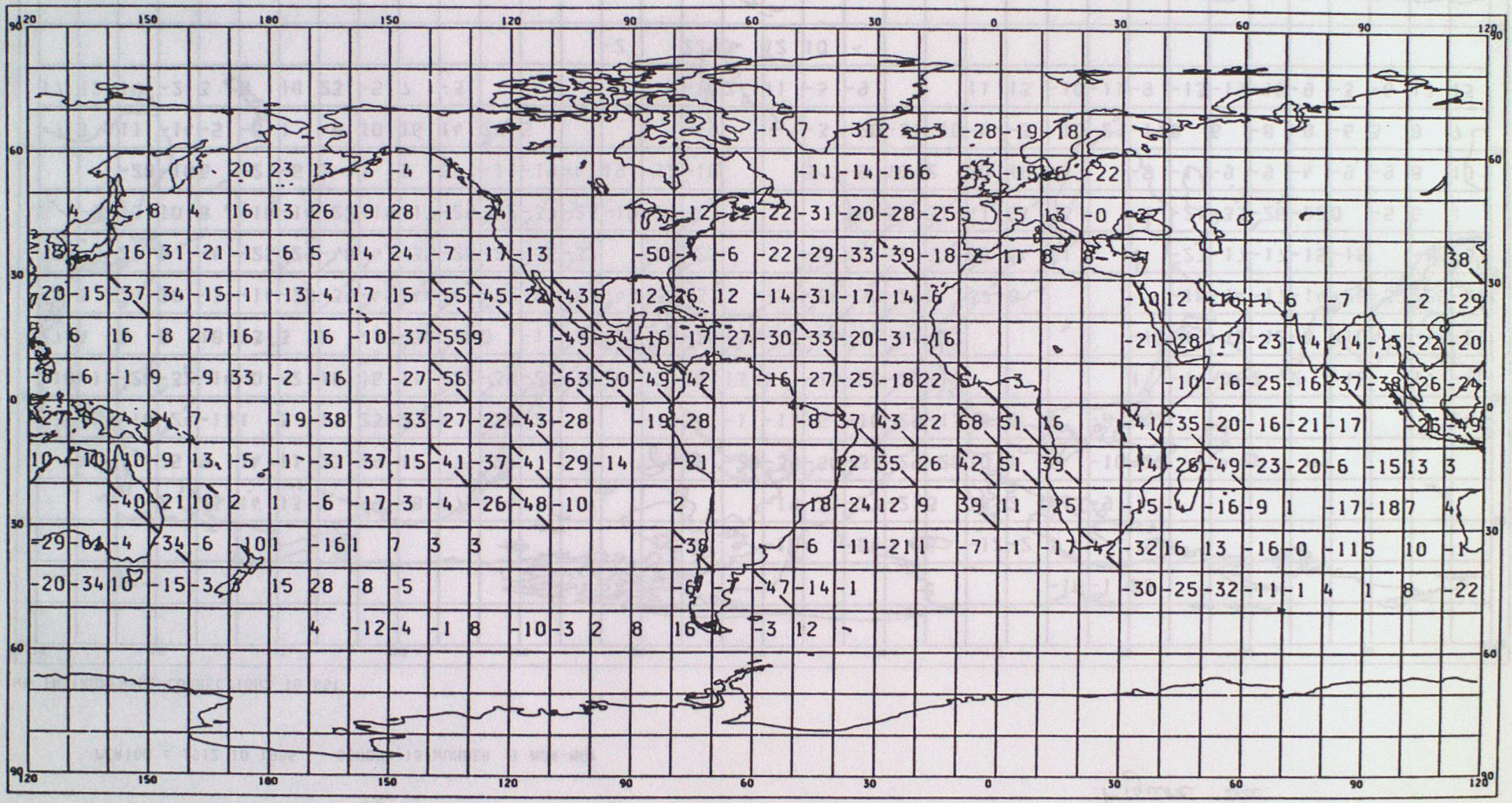

Figure 5c.

PERIOD = 1949 TO 1985 . SEASON IS NUMBER 1 MAR-MAY

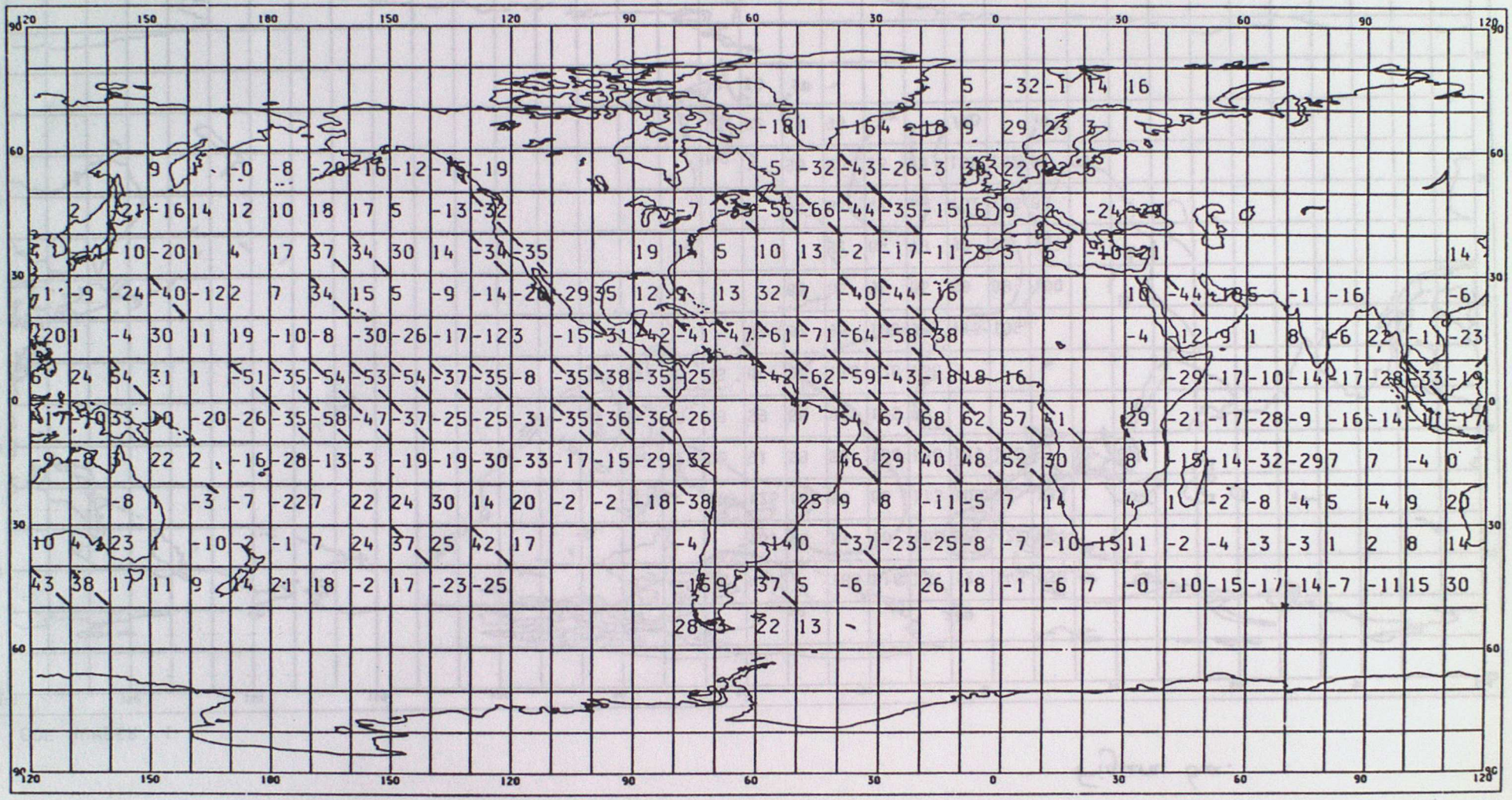

Figure 6a.

EOF NUMBER 1

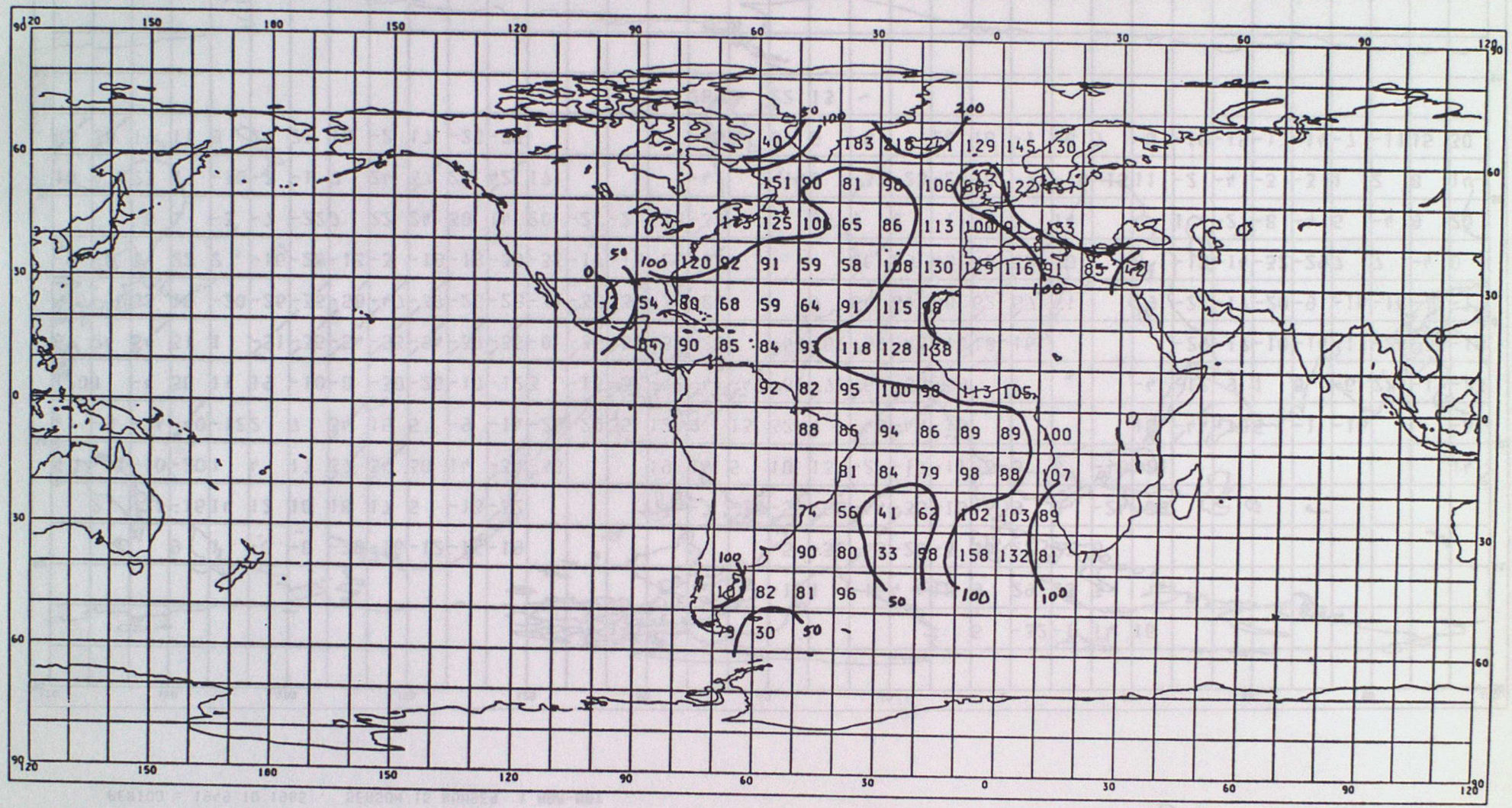

AT1 x 1000

Figure 6b.

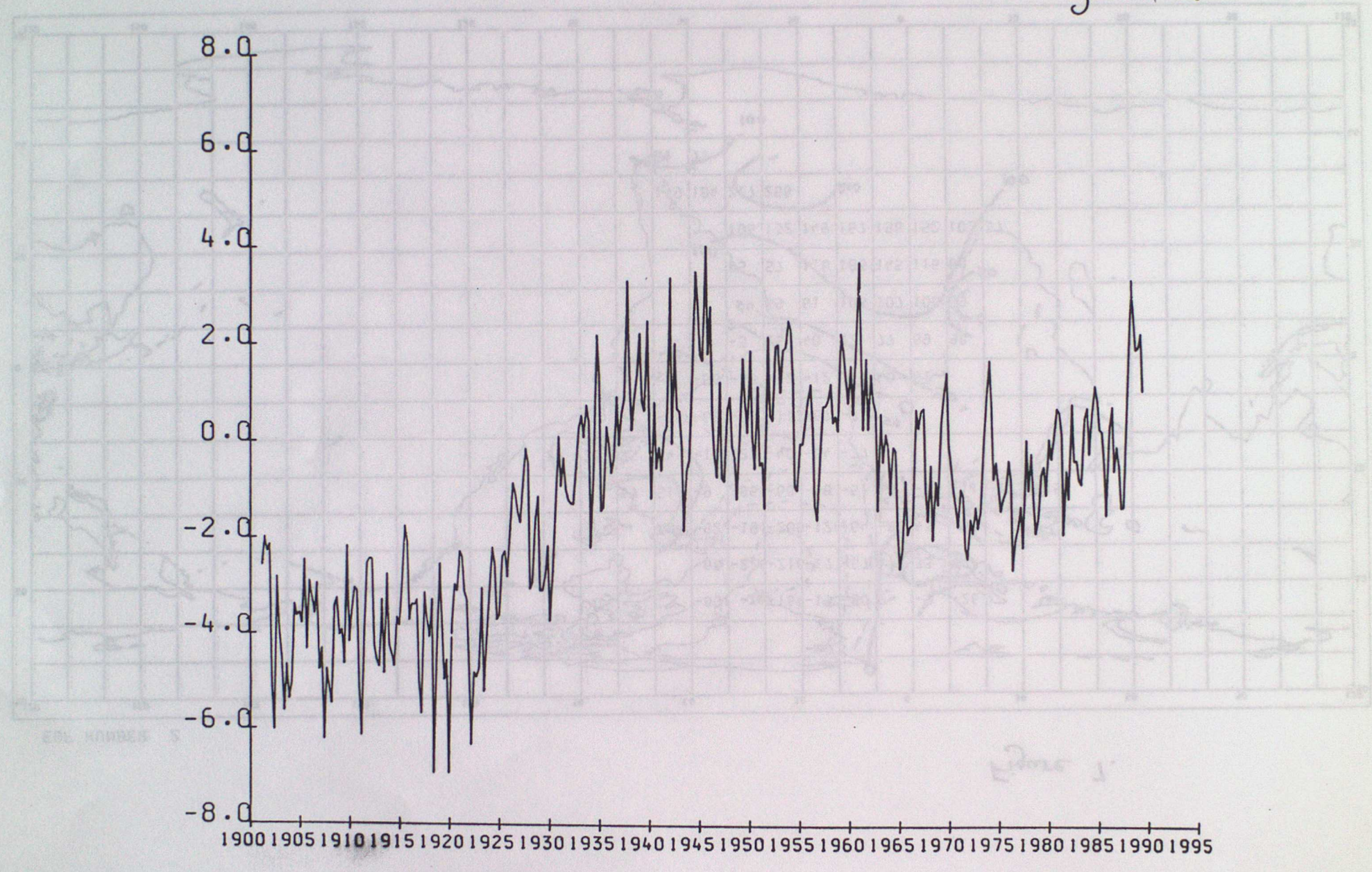

Figure 7.

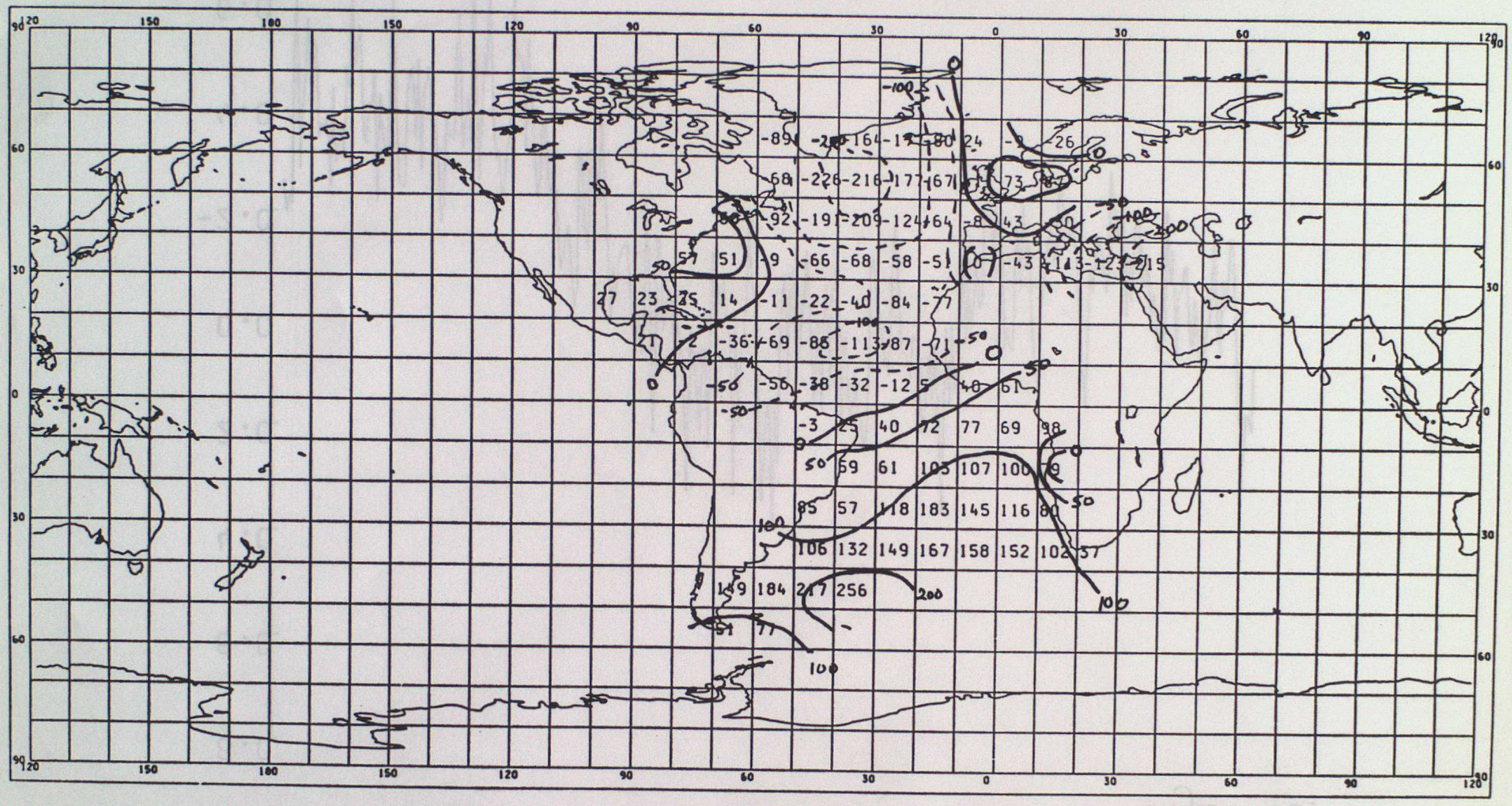
EOF NUMBER 2
120
150
180
150
120
90
60
30
0
30
60
90
120
90
60
30
0
30
60
90
-100
-89
-26
68
-226
-216
177
167
73
92
-191
-209
-124
64
-8
43
57
51
-9
-66
-68
-58
-51
-43
27
23
14
-11
-22
-40
-84
-77
-36
-69
-88
-113
87
71
-50
-56
-38
-32
-12
5
40
61
-3
25
40
72
77
69
98
59
61
105
107
100
85
57
118
183
145
116
106
132
149
167
158
152
102
37
169
184
217
256
200
100

Figure 8a

EOF NUMBER 3

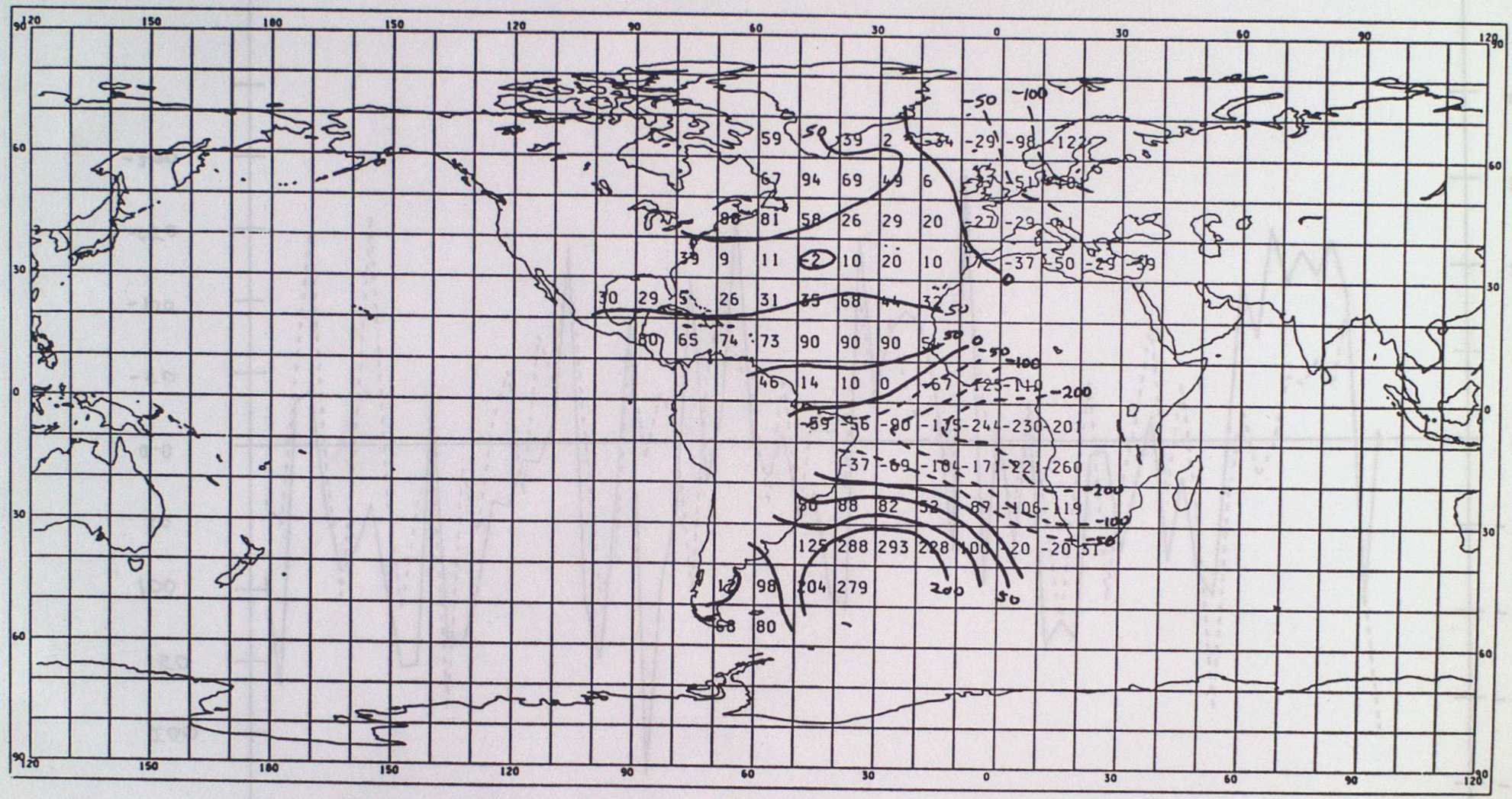

N. NORDESTE RAIN

STANDARDISED ANOMALY x 100

Figure 8b.

AT3 x -1000

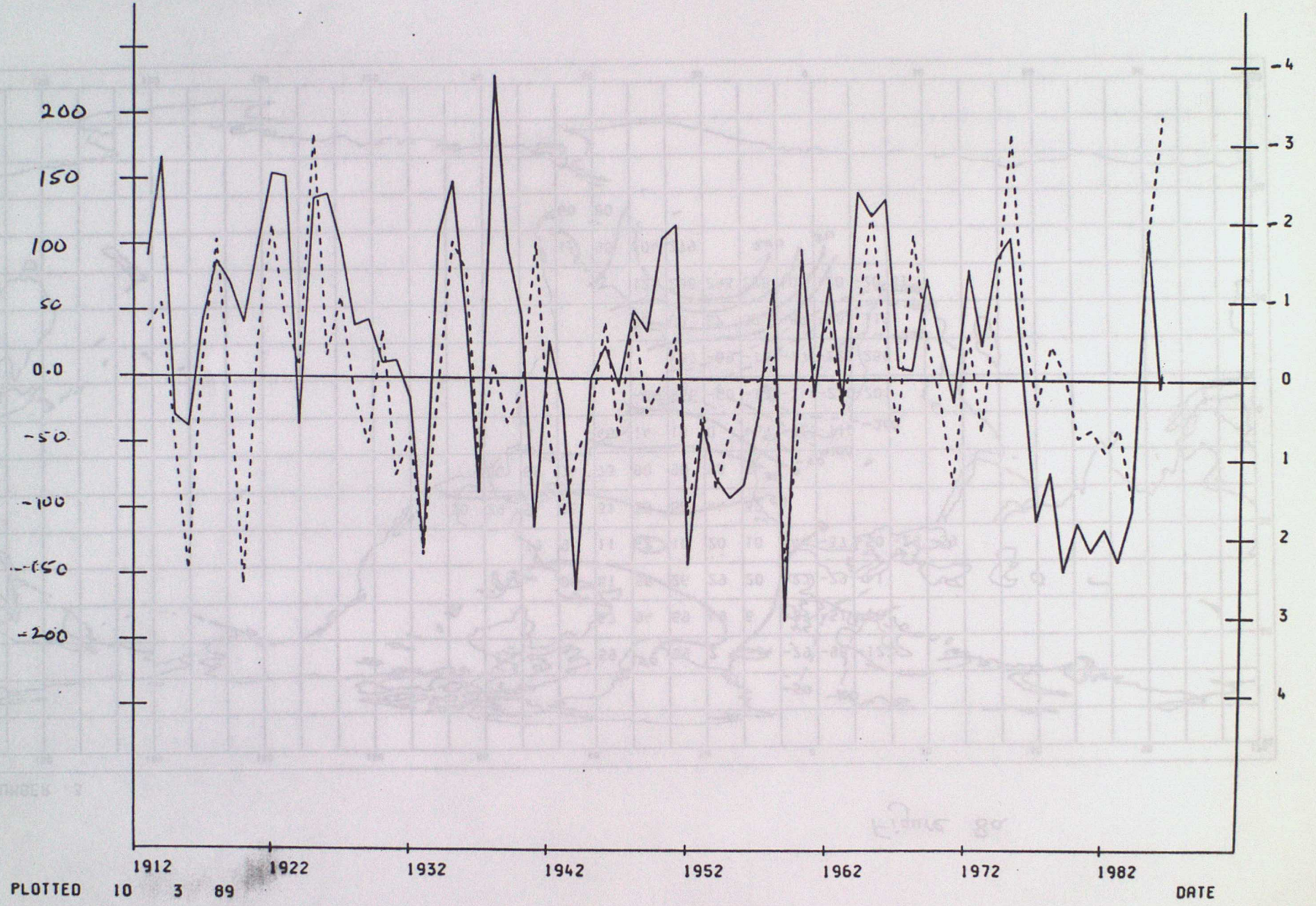

Figure 9a

EOF NUMBER 1

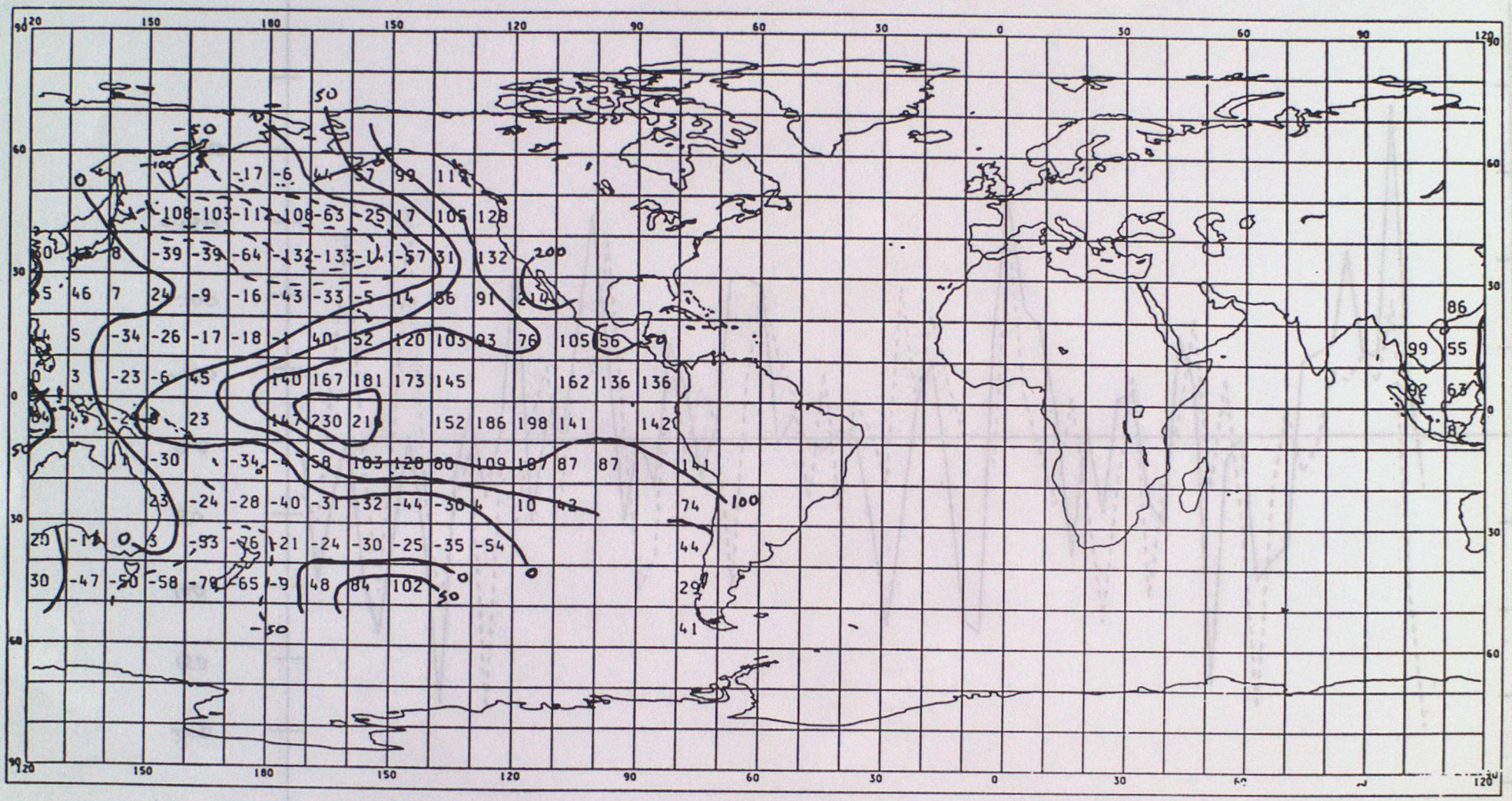

Figure 9b.

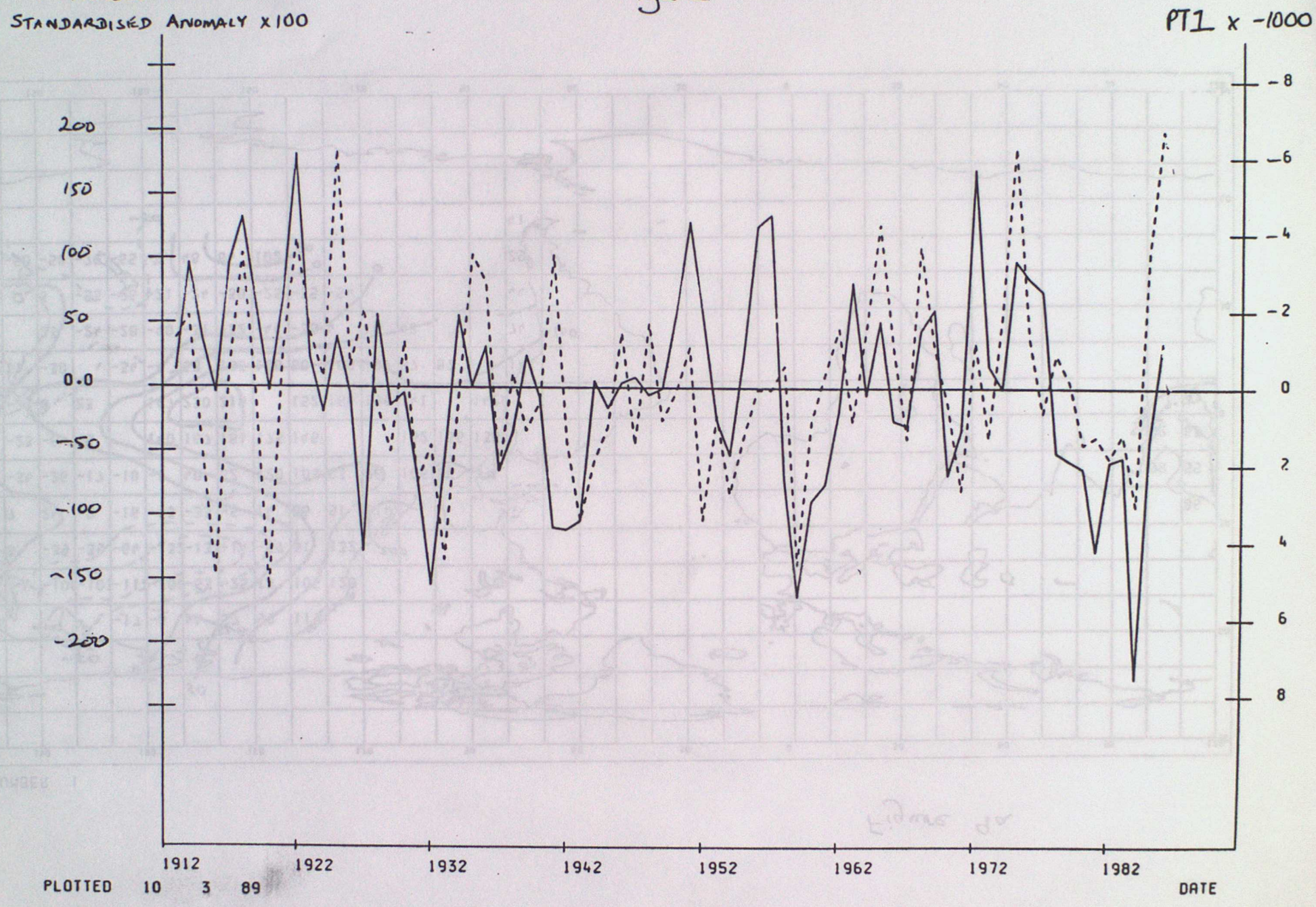
N. NORDESTE RAIN
STANDARDISED ANOMALY x100
PTI x -1000
200
150
100
50
0.0
-50
-100
-150
-200
-8
-6
-4
-2
0
2
4
6
8
1912
1922
1932
1942
1952
1962
1972
1982
PLOTTED 10 3 89
DATE

Figure 10.

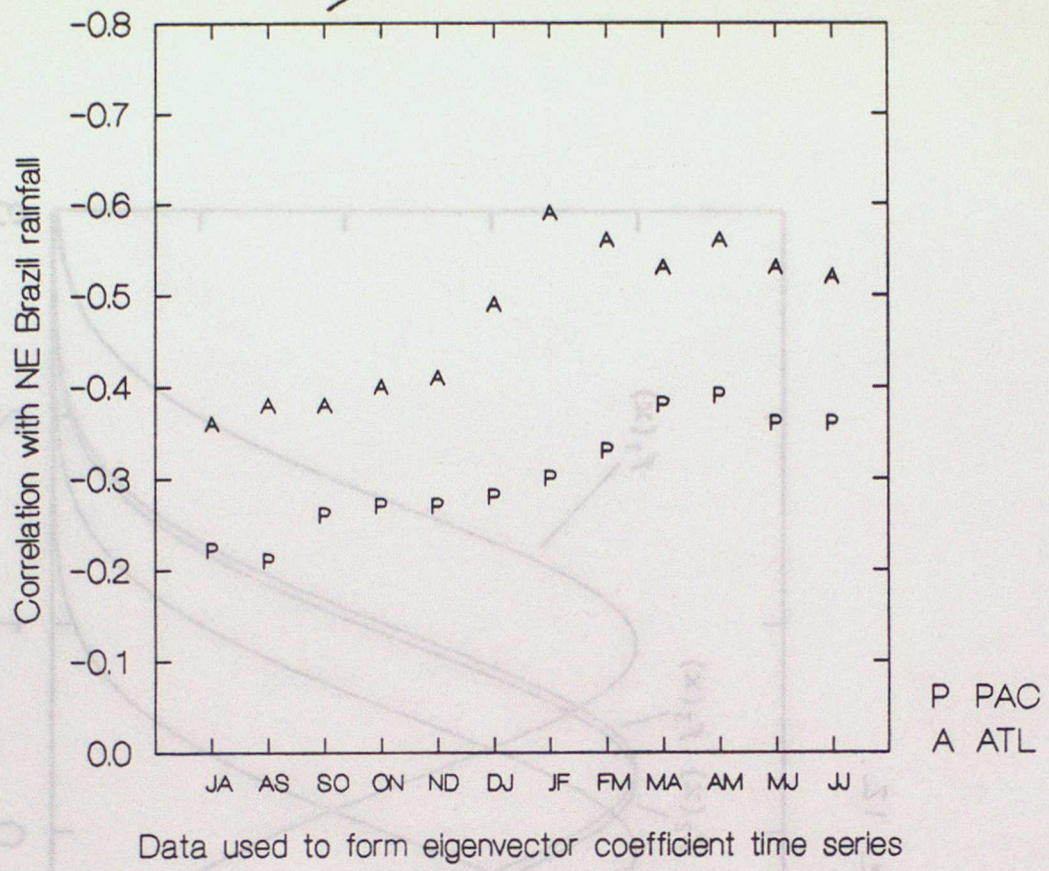

Figure 11.

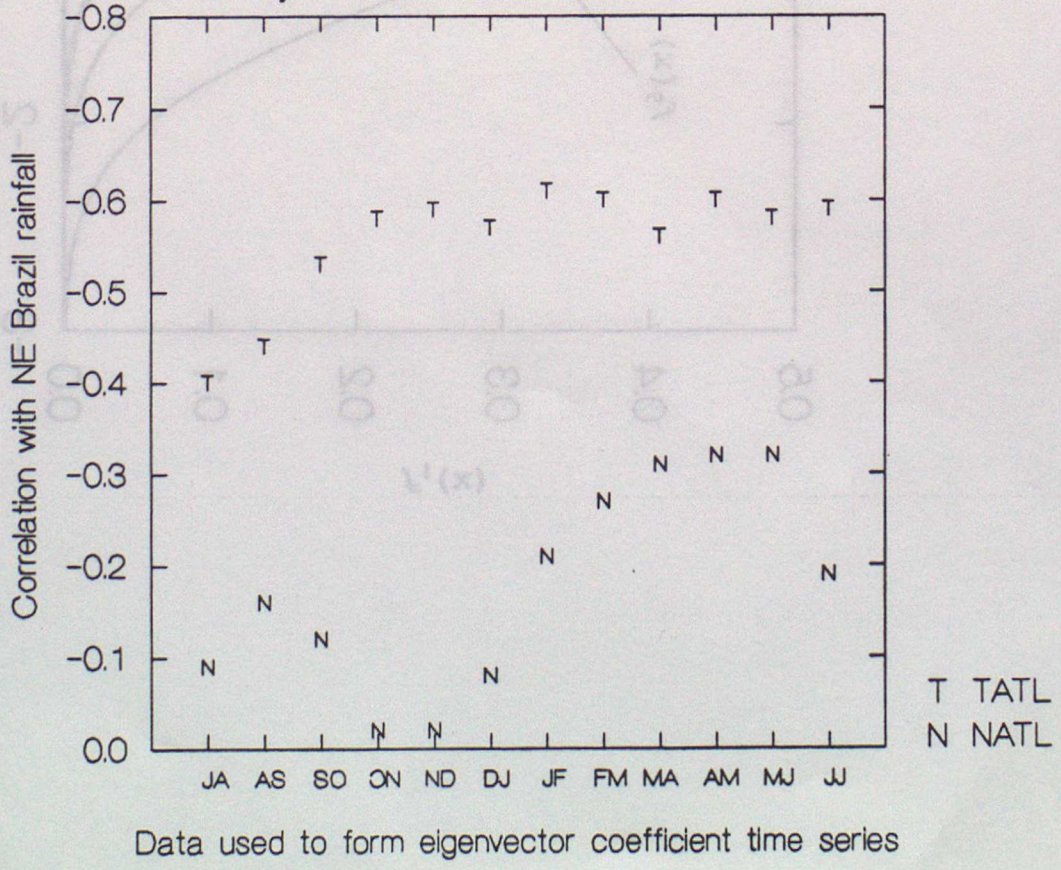

Figure 12.

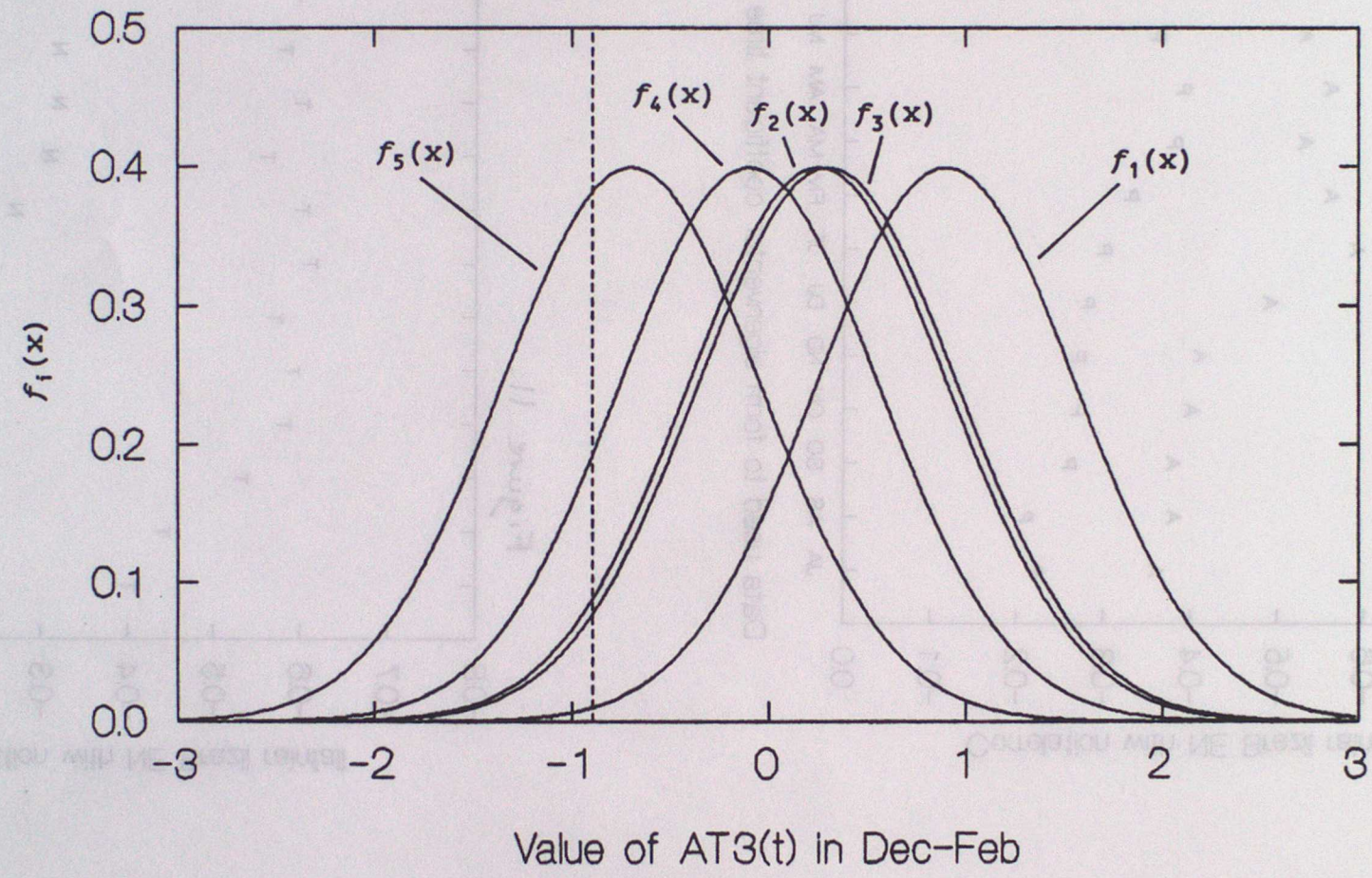
0.5
0.4
0.3
0.2
0.1
0.0
$f_i(x)$
$f_5(x)$
$f_4(x)$
$f_2(x)$
$f_3(x)$
$f_1(x)$
-3
-2
-1
0
1
2
3
Value of AT3(t) in Dec-Feb

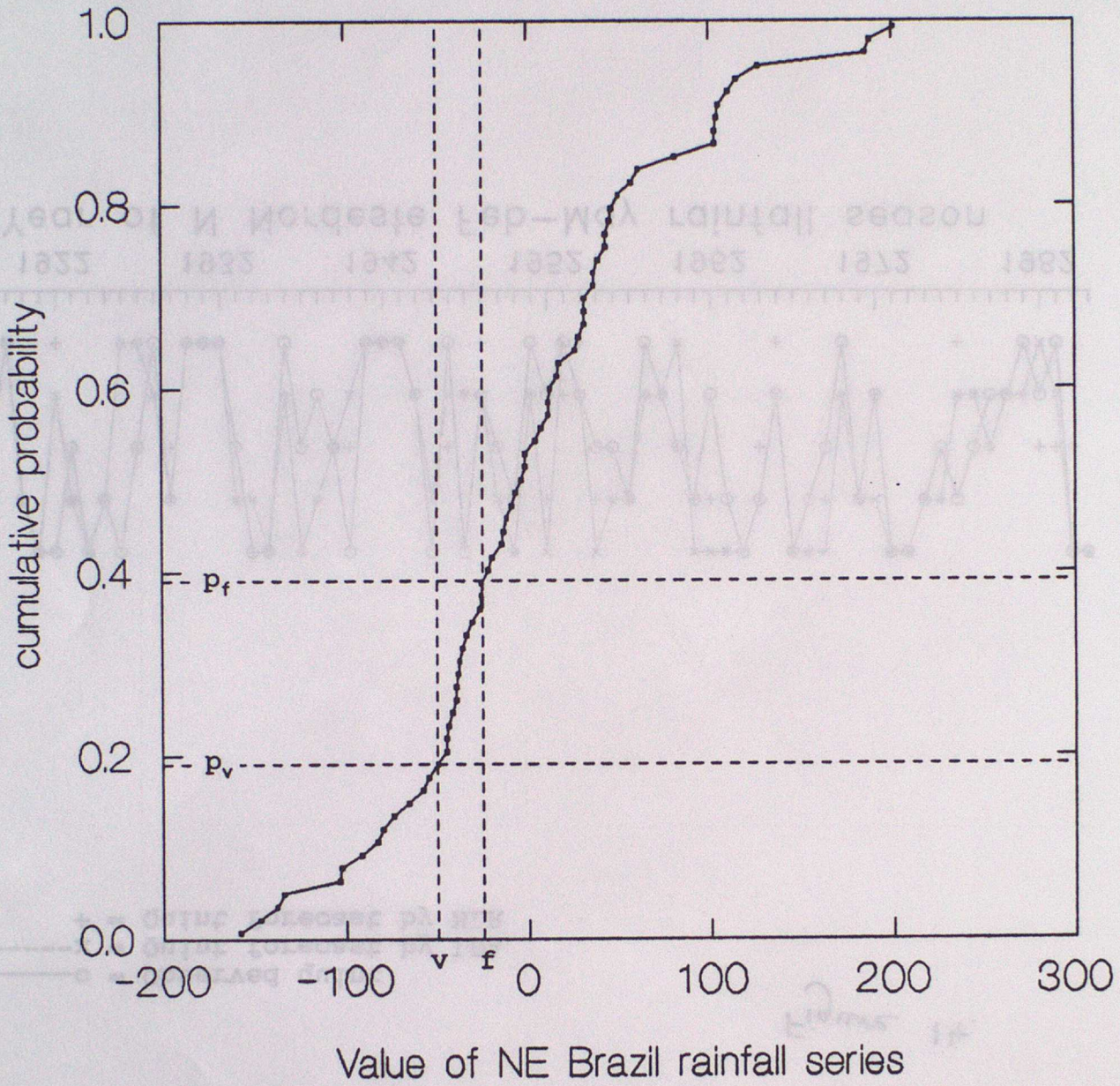
1.0
0.8
0.6
0.4
0.2
0.0
cumulative probability
p_f
p_v
v
f
-200
-100
0
100
200
300
Value of NE Brazil rainfall series

Figure 13.

Figure 14.

key: o———o = Observed quint
x-------x = Quint forecast by LDA
+ + = Quint forecast by MLR

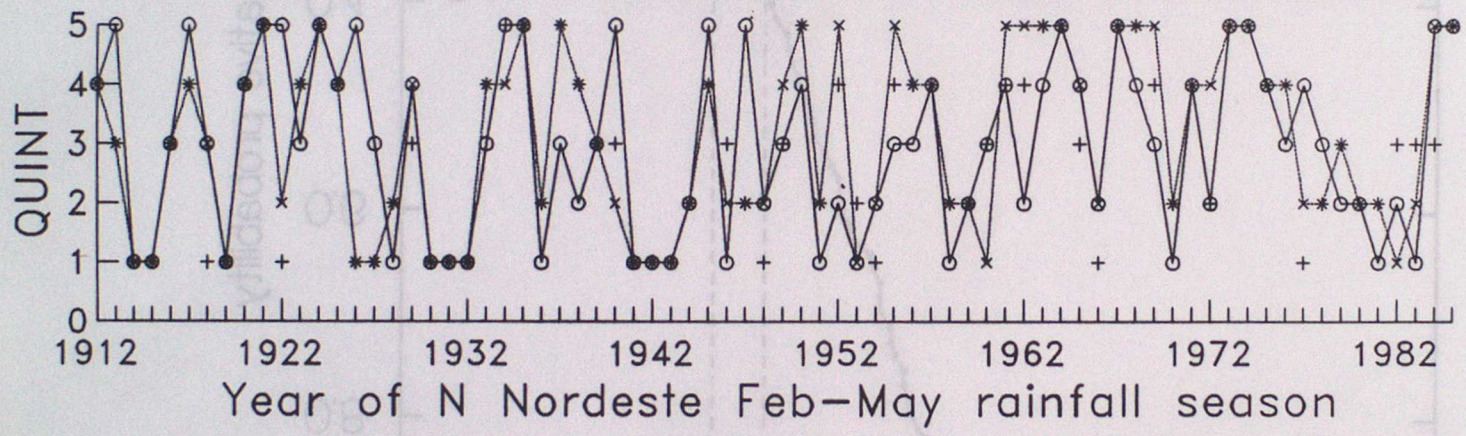

INDEX TO LONG-RANGE FORECASTING AND CLIMATE RESEARCH SERIES

1) THE CLIMATE OF THE WORLD - Introduction and description of world climate.
by C K Folland (March 1986)

2) THE CLIMATE OF THE WORLD - Forcing and feedback processess.
by C K Folland (March 1986)

3) THE CLIMATE OF THE WORLD - El Nino/Southern Oscillation and the Quasi-biennial Oscillation.
by C K Folland (March 1986)

4) THE CLIMATE OF THE WORLD - Climate change: the ancient earth to the 'Little Ice Age'.
by C K Folland

5) THE CLIMATE OF THE WORLD - Climate change: the instumental period.
by C K Folland (March 1986)

6) THE CLIMATE OF THE WORLD - Carbon dioxide and climate (with appendix on simple climate models).
by C K Folland (March 1986)

7a) Sahel rainfall, Northern Hempishere circulation anomalies and worldwide sea temperature changes, (To be published in the Proceedings of the "Pontifical Academy of Sciences Study Week", Vatican, 23-27 September 1986).
by C K Folland, D E Parker, M N Ward and A W Colman (September 1986)
(Amended July 1987)

8) Lagged-average forecast experiments with a 5-level general circulation model.
by J M Murphy (March 1986)

9) Statistical Aspects of Ensemble Forecasts.
by J M Murphy (July 1986)

10) The impact of El Nino on an Ensemble of Extended-Range Forecasts.
(Submitted to Monthly Weather Review)
by J A Owen and T N Palmer (December 1986)

11) An experimental forecast of the 1987 rainfall in the Northern Nordeste region of Brazil.
by M N Ward, S Brooks and C K Folland (March 1987)

12) The sensitivity of Estimates of Trends of Global and Hemispheric Marine Temperature to Limitations in Geographical Coverage.
by D E Parker (April 1987)

13) General circulation model simulations using cloud distributions from the GAPOD satellite data archive and other sources.
by R Swinbank (May 1987)

14) Similation of the Madden and Julian Oscillation in GCM Experiments.
by R Swinbank (May 1987)

15) Numerical simulation of seasonal Sahel rainfall in four past years using observed sea surface temperatures.
by J A Owen, C K Folland and M Bottomley (April 1988)

16) Not used

17) A note on the use of Voluntary Observing Fleet Data to estimate air-sea fluxes.
by D E Parker (April 1988)

18) Extended-range prediction experiments using an 11-level GCM
by J M Murphy and A Dickinson (April 1988)

19) Numerical models of the Raingauge Exposure problems - field experiments and an improved collector design.
by C K Folland (May 1988)

20) An interim analysis of the leading covariance eigenvectors of worldwide sea surface temperature anomalies for 1901-80.
by C K Folland and A Colman (April 1988)

21) Prospects for long range forecasting for the United Kingdom.
by A Dickinson and C K Folland (July 1988)

22) CLIMATE OF THE WORLD (Restricted Issue)
1. Introduction to world climate
2. Description of world climate
by C K Folland and D E Parker (July 1988)

23) CLIMATE OF THE WORLD (Restricted issue)
3. Climatic forcing and feedback processes.
I. Forcing from above.

4. Climatic forcing and feedback processes.
II. Interactions with land surface
by C K Folland and D E Parker (July 1988)

24) CLIMATE OF THE WORLD (Restricted Issue)
5. Ocean-atmosphere interaction
by D E Parker and C K Folland (July 1988)

25) CLIMATE OF THE WORLD (Restricted Issue)
6. The El Nino/Southern Oscillation, the Quasi-Biennial Oscillation, and the 30-60 day variations.
by C K Folland and D E Parker (July 1988)

26) CLIMATE OF THE WORLD (Restricted Issue)
7. A review of palaeoclimate from the early Earth to the Pleistocene ice ages

8. Climate from the late glacial to the "Little ice age"
by C K Folland and D E Parker (July 1988)

27) CLIMATE OF THE WORLD 9. Climatic change in the instrumental period
(Restricted Issue) by D E Parker and C K Folland (July 1988)

28) CLIMATE OF THE WORLD 10. Carbon dioxide and other greenhouse gases, and
(Restricted Issue) climatic variation
(with appendix on simple climate models).
by D E Parker, C K Folland and D J Carson
(July 1988)

29) Comparison of corrected sea surface and air temperature for the globe and the hemispheres 1856-1988 - Presented at the 12th Annual Climate diagnostics Workshop, Boston USA 31 Oct - 4 Nov 1988.
by C K Folland and D E Parker (November 1988)

30) Development of a Sahel rainfall series using CLIMAT data
by A W Colman (December 1988)